Author Response to Reviews of

A dense network of cosmic-ray neutron sensors for soil moisture observation in a pre-alpine headwater catchment in Germany

Benjamin Fersch et al.

RC: *Reviewer Comment*,   AR: *Author Response*,   ☐ Manuscript text

Dear Referees,

we would like to thank you very much for your positive comments and constructive suggestions to our manuscript. Here, we compiled our responses for the comments of each of the referees into one single document and outlined the corresponding changes made to the manuscript. We hope that our response together with the revision of the manuscript sufficiently addresses the referees' concerns.

Kind regards,

Benjamin Fersch

on behalf of the author team

1. Referee #1

1.1. Title

> A dense network of cosmic-ray neutron sensors for soil moisture observation in a pre-alpine headwater catchment in Germany

RC: *I am not sure if the title of the paper is a good representation of the content as there is just as much data on meteorology and alternative soil moisture information as there is on CRNS measurements. Not sure how best to capture the breadth of observations but perhaps a title along the lines of the following might be better...*

"A dense network of cosmic-ray neutron sensors for soil moisture observation in a pre-alpine headwater catchment in Germany including supplementary meteorological and hydrological observations"

or

"A dense network of cosmic-ray neutron sensors and supplementary measurements for soil moisture observation in a pre-alpine headwater catchment in Germany"

AR: *We thank the referee for the suggestion. We would like to propose the following changed title: "A dense network of cosmic-ray neutron sensors for soil moisture observation in a highly instrumented pre-alpine headwater catchment in Germany".*

1.2. Availability of a soil moisture product

RC: ***The datasets are well organised with suitable metadata and data structures used throughout. I would like to have seen a version of the CRNS static data with an estimate of soil moisture data using a predefined approach. I realise techniques are evolving and the key focus is on CRNS processing options, but this would provide an off-the-shelf option for some users who just want some measure of soil moisture for analysis (i.e. hydrological model, satellite cal/val). This may increase data utilisation. As it stands the raw counts and all of the data required for corrections and processing are provided, but users with little experience in the CRNS field may be a little reluctant to process the data themselves.***

AR: *We certainly understand the referee's concern that the presented data would not be helpful for users with little experience. Yet, the referee pointed out himself that the retrieval of a soil moisture product from neutron count rates is still evolving and not trivial. The aim of this data publication is to provide a data set to the research community that can be used for soil moisture estimation at varying levels of complexity. Adding any preliminary or "first-order" soil moisture product as part of the published data set would not be a valuable service to the community. Providing an in-depth analysis, on the other hand, is certainly beyond the scope of this publication. Instead, we are currently working on an extensive study that explores options for soil moisture estimation at the level of individual probes, but, more importantly, on the consistent interpolation of soil moisture across the study area. As part of that ongoing study, we also aim at providing a soil moisture product which will then be adequately documented and validated as part of the corresponding publication.*

1.3. Line 8

RC: ***Change 'that network' to 'this network'***

AR: *Changed.*

1.4. Line 10

RC: ***change to '...allow users to...'***

AR: *Changed.*

1.5. Line 19

RC: ***change to '...EU-DAT and is split into two subsets...'***

AR: *Changed to: "EUDAT Collaborative Data Infrastructure (EUDAT), and is split into two subsets:"*

1.6. Line 19

RC: ***1st hyperlink includes first part of reference and does not work***

AR: *We are sorry that the hyperlink did not appear to work for the referee. We double-checked it with different pdf reader formats and it worked as expected. We would like to ask the reviewer to double check the link as well, and we hope for a final solution of the issue during the process of typesetting.*

1.7. Line 29

RC: *maybe spell out TDR and TDR first time through*

AR: *We assume the referee meant "FDR and TDR". We spelled out both at first time use in the revised version.*

1.8. Line 31

RC: *do you mean support volume*

AR: *Correct. We changed "support" to "support volume".*

1.9. Line 36

RC: *add 'are' between 'and' and 'thus*

AR: *Added.*

1.10. Line 39

RC: *It might be less clunky to just say they have poor temporal resolution.*

AR: *We thank the referee, but we would prefer to keep the sentence as it is since such datasets do not actually have a temporal "resolution", but could just be snapshots at arbitrary points in time. Thank you, we changed "infrequent measurement intervals" to "poor temporal resolution".*

1.11. Line 44

RC: *Not sure describing the footprint as exponentially shaped is a good description. The footprint declines radially with distance from the CRNS – its more bell shaped or declines exponentially with distance from the CRNS.*

AR: *Thank you for pointing this out, we have indeed described the shape inappropriately. The shape is actually very complex and not easy to describe in short. Since those details are not relevant here, we think that the provided reference is sufficient and we removed the term "exponentially-shaped" from the text.*

1.12. Line 48

RC: *'...presented the first...'*

AR: *Changed.*

1.13. Line 58

RC: *change to "...monitoring exists and these use various gases..."*

AR: *Changed.*

1.14. Line 87

RC: *suggest deleting after the :*

AR: *We understand the suggestion. Yet, we prefer to keep the two items after the column as it helps guiding the*

reader through what follows next. We replaced the colon with "such as".

1.15. Line 88

RC: *needs rewording - does not make sense as is*

AR: *Thank you, we changed the sentence:*

> The term *Roving CRNS* ~~involves~~ stands for the utilization of mobile CRNS sensors ~~, have~~ to increase the spatial extent of soil moisture measurements. .

1.16. Line 96

RC: *change 'of' to 'in'*

AR: *Changed.*

1.17. Line 130

RC: *change 'had' to 'have'*

AR: *Changed.*

1.18. Line 149

RC: *delete 'however'*

AR: *Deleted.*

1.19. Line 156

RC: *By backbone do you mean existing long-term datasets? If so suggest changing.*

AR: *Changed "backbone" to "long-term".*

1.20. Line 160

RC: *change 'could identify' to 'identified'*

AR: *Changed.*

1.21. Line 170

RC: *insert 'this was' between 'and' and 'followed'*

AR: *Added.*

1.22. Line 213

RC: *Do you mean back ground?*

AR: *We removed the word "backbone".*

1.23. Figure 2

RC: *Figure 2 is not referenced in the text.*

AR: *We changed the text as follows: "Tab. 2 gives an overview of all stationary CRNS sensors that were used during the campaign. Fig. 2 illustrates the proportions of the different sensor models."*

1.24. Fig. 3 caption

RC: *Use "Note: y-axis scaling differs between plots"*

AR: *Changed.*

1.25. Line 361 & Line 362

RC: *inverted commas wrong*

AR: *Corrected.*

1.26. Line 374

RC: *Needs to be reworded for clarity. What is being constrained? Models?*

AR: *We suggest to replace "but also allows to better constrain" by "it also informs about":*

> The vertical distribution pattern is not only affecting the vertical CRNS footprint (Köhli et al., 2015), but ~~also allows to better constrain~~ it also informs about vertical water movement and thus groundwater recharge (Baroni et al., 2018).

1.27. Line 386

RC: *change to "A large number of manual soil moisture measurements were carried out from June 25 to 26, 2019 and these were useful for increasing the spatial coverage of the continuously-recorded soil moisture data, enabling the calibration of the moisture sensors and obtaining basic soil properties (bulk density, residual water content, organic matter content, texture).*

AR: *Adopted.*

1.28. Line 475

RC: *change 'is' to 'was*

AR: *Changed.*

1.29. Line 493

RC: *'on top of'*

AR: *Changed.*

1.30. Line 567

 RC: *remove 'yet' and 'already'*

 AR: *Removed.*

1.31. Line 578

 RC: *delete 'already'*

 AR: *Deleted.*

1.32. Line 600

 RC: *change to "...allow users to..."*

 AR: *Changed.*

2. Referee #2

2.1. Introduction

RC: *I think the context chosen by the authors to justify the choice of area is slightly incomplete (or maybe slightly misleading). Reading the relevant sections of the manuscript, it gives the impression that this choice was because typical applications of cosmic-ray sensors are either done for single (isolated) sites or for large-scale continental/national networks, which consequently misses this overlapping aspect of multiple measurements at the same 1 sq-km (grid) area (note that the area represents a tiny fraction of the 55 sq-km Rott catchment). The nature of single sites of large networks is continuous monitoring capability whereas here the data describes a short-term summer campaign (from late-April to early-July). There is nothing majorly wrong with the text but given that this is short campaign, framing the paper more towards the importance of short-term intensive campaigns would, in my opinion, make the paper present better the motivation for this dataset. Authors can cite similar work done for other products such as SMOSMANIA and SMAPEx campaigns, for example. In addition, an area of 1 sq-km is probably related to very small catchments, and the context would probably be better linked to understanding spatial heterogeneity for high-resolution soil moisture applications. I am surprised to see the authors failed to cite seminal work by Roger Grayson, Andrew Western, and Gunther Bloschl in the 1990s that tackle this high-resolution measurement problem with very interesting and impactful results to the hydrological community.*

AR: *We thank the referee for this thoughtful comment. Yet, we tend to disagree with the view that the prime feature of the presented campaign was its short-term character - in comparison to long-term national scale networks. At least we interpret the following comment accordingly: "[...] given that this is a short campaign, framing the paper more towards the importance of short-term intensive campaigns would, in my opinion, make the paper present better the motivation for this dataset." In our view, however, the prime feature of this campaign was the high spatial density of CRNS sensors in a study area characterised by large heterogeneity of land use, soil, and soil moisture. That spatial density is motivated, on the one hand, by the aim to cover root zone soil moisture dynamics at the small catchment scale, and, on the other hand, by the aim to represent the spatial variability of soil moisture at that scale, and to use the overlap of CRNS footprints for that purpose. As soon as you place CRNS probes so far from each other that their footprints do not overlap anymore, the retrieval of spatial patterns is "reduced" to the problem of spatial interpolation. However, as the footprints overlap, there is the potential to extract additional spatial information from the fact that the same area is covered by different probes (similar to the idea of a geophysical inversion). We have tried to explain these aspects in ll. 121–125 of the original manuscript.*

So while we appreciate the comment, we think that the short-term character of this campaign is not its prime feature nor its motivation. The duration was rather constrained by resources. However, we have already started to establish a dense network of 12 CRNS sensors near Potsdam that is designed at least for a medium-term operation (i.e. several years).

Based on the above argument, we would also prefer not to explicitly cite the suggested references on SMOSMANIA and SMAPEX. While SMAPEX was specifically geared towards understanding soil moisture variability inside the SMAP footprint scale (i.e. 10–30 km), SMOSMANIA is about soil moisture monitoring at 21 locations as part of the national scale meteorological observation network RADOME (Meteo France). SMOS and SMAP themselves are already referred to in the overview papers we cited in section 1.1 (Wang and Qu, 2009; Mohanty et al., 2017). Yet, we thank the referee for suggesting Blöschl and Grayson who of course cannot be cited too often. In the revised version, we refer to "Blöschl, G., R. Grayson (2000): Spatial Observations and Interpolation. In: Blöschl, G., R. Grayson (Eds.): Spatial Patterns in Catchment Hydrology

- Observations and Modelling, Cambridge University Press, pp. 17-50" in l. 30 of the original manuscript.

2.2. Figure numbering

RC: *In many instances throughout the paper, I don't understand why the manuscript jumps to figures without following a common numerical order (introduces Figures 1 previously, then refers to Figure 9 here; then refers to Fig 3 later on; Fig 2 is not referred in the text before showing up in the manuscript, etc...). This makes reading through the manuscript a bit more difficult.*

AR: *We apologize for any inconvenience, but using the Copernicus tex template, we could not influence the actual placement of the figures in the manuscript draft. We will take additional care of this issue during the copy-editing phase. As for Fig. 2, we have now referenced it in line 229. Fig. 9 constitutes an exception, as it is used both for illustrating the temporal coverage and presenting example. Because the focus is on the latter, it is placed closer to this sections.*

2.3. Is the CRNS technique still "novel"?

RC: *The cosmic-ray neutron sensing technique for soil moisture application is now more than 10 years old. I'd strongly encourage the authors and the community, in general, to stop using words like "emerging", "novel", "promising", etc... to describe the technique as these statements now read a bit outdated.*

AR: *We agree with your view that the CRNS method is being used for various applications and that – since its broader introduction in 2010 – it became a certain standard in environmental monitoring. On the other hand, there are still many open questions in the setup and processing of the measurements, compared to, e.g., TDR technology. Moreover, the full potential of CRNS applications has not yet been exploited, such as, e.g., large scale coverage. In the text we have now adapted the wording to better acknowledge the current situation and successful history of the technique.*

2.4. Lines 70-71

RC: *Perhaps the authors can include the citation to previous studies that have altered the values of the 'a' coefficients in an attempt to improve the estimated soil moisture signal from the sensor:*

Rivera Villarreyes, C. A., Baroni, G., & Oswald, S. E. (2011). Integral quantification of seasonal soil moisture changes in farmland by cosmic-ray neutrons. Hydrol. Earth Syst. Sci., 15(12), 3843–3859. https://doi.org/10.5194/hess-15-3843-2011

Iwema, J., Rosolem, R., Baatz, R., Wagener, T., and Bogena, H. R.: Investigating temporal field sampling strategies for site-specific calibration of three soil moisture–neutron intensity parameterisation methods, Hydrol. Earth Syst. Sci., 19, 3203–3216, https://doi.org/10.5194/hess-19-3203-2015, 2015.

Heidbüchel, I., Güntner, A., and Blume, T.: Use of cosmic-ray neutron sensors for soil moisture monitoring in forests, Hydrol. Earth Syst. Sci., 20, 1269–1288,https://doi.org/10.5194/hess-20-1269-2016, 2016.

AR: *Thank you for suggesting additional papers about the a_i parameters. We reformulated the sentence:*

> The ~~shape~~ parameters a_0, a_1, and a_2 ~~could be adapted to specific local conditions, but they have also proven~~ have proved to be robust in ~~many previous studies~~ their original formulation across multiple CRNS sites (Desilets et al., 2010; Evans et al., 2016; Schrön et al., 2017, among others), while few locations apparently work better with different values (Rivera Villarreyes et al., 2011; Iwema et al., 2015; Heidbüchel et al., 2016) .

2.5. Figure 6

RC: *There is just too much information in this figure. What is the main purpose of the figure? Do the authors need to show all numbers on those maps? Do they need to show all maps?*

AR: *Figure 6 shows the tracks and patterns of the roving campaign. We have replaced the IDs of the CRNS-probes with simple symbols for clarity. However, we intend to show the maps for all dates to illustrate the spatiotemporal coverage of the rover campaigns and the resulting qualitative spatial patterns of soil moisture.*

2.6. Example application

RC: *As an example of application, the authors could easily have identified how similar or different the measurements are (20+ sensors in a 1 sq-km area seems a bit too much for me). Perhaps they could either look at the different CDF for each measurement and determine if they theoretically come from the same or different distribution using the Kolmogorov-Smirnov test; or apply some temporal stability analysis (???)*

AR: *We thank the referee for this interesting suggestion, which we will try to incorporate in our ongoing analysis of the data. Without doubt, there are countless other analyses that could be performed with the presented data. Therefore, we are happy to provide these data to the community. However, we cannot and do not intend to present any exhaustive analysis in this paper. In accordance to the ESSD journal guidelines, we are focusing on the documentation of the dataset only. Our presented application is merely one of many examples of how this dataset could be used.*

3. General Remarks

- In the submitted version of the data and the manuscript, we provided measurements of four different Bonner Spheres from June to July. However, in July four additional Bonner Spheres were installed (8 in total) which we would like to add also to the revised version of the manuscript. The additional data could help to even better resolve the energy spectrum of the cosmic-ray neutrons at the site. We updated Fig. 5 and the corresponding text accordingly.

- The dataset on EUDAT for part I has been updated an is now available under the DOI
  `https://doi.org/10.23728/b2share.282675586fb94f44ab2fd09da0856883`.
  Accordingly, although unchanged, the part II dataset is now available from the DOI
  `https://doi.org/10.23728/b2share.bd89f066c26a4507ad654e994153358b`

A dense network of cosmic-ray neutron sensors for soil moisture observation in a highly instrumented pre-alpine headwater catchment in Germany

Benjamin Fersch[1], Till Francke[2], Maik Heistermann[2], Martin Schrön[3], Veronika Döpper[4],
Jannis Jakobi[5], Gabriele Baroni[2,6], Theresa Blume[7], Heye Bogena[5], Christian Budach[2], Tobias Gränzig[4],
Michael Förster[4], Andreas Güntner[7,2], Harrie-Jan Hendricks-Franssen[5], Mandy Kasner[3],
Markus Köhli[8,9], Birgit Kleinschmit[4], Harald Kunstmann[1,10], Amol Patil[10], Daniel Rasche[7,2],
Lena Scheiffele[2], Ulrich Schmidt[8], Sandra Szulc-Seyfried[2], Jannis Weimar[8], Steffen Zacharias[3],
Marek Zreda[11], Bernd Heber[12], Ralf Kiese[1], Vladimir Mares[13], Hannes Mollenhauer[3], Ingo Völksch[1],
and Sascha Oswald[2]

[1]Karlsruhe Institute of Technology, Campus Alpin (IMK-IFU), Kreuzeckbahnstraße 19, 82467 Garmisch-Partenkirchen, Germany
[2]Institute of Environmental Science and Geography, University of Potsdam, Karl-Liebknecht-Straße 24–25, 14476 Potsdam, Germany
[3]UFZ – Helmholtz Centre for Environmental Research GmbH, Dep. Monitoring and Exploration Technologies, Permoserstr. 15, 04318, Leipzig, Germany
[4]Technical University of Berlin, Geoinformation for Environmental Planning Lab, Straße des 17. Juni 135, 10623 Berlin, Germany
[5]Agrosphere IBG-3, Forschungszentrum Jülich GmbH, Leo-Brandt-Straße, 52425 Jülich, Germany
[6]Department of Agricultural and Food Sciences, University of Bologna, Viale Fanin 50, 40127 Bologna, Italy
[7]GFZ German Research Centre for Geosciences, Section Hydrology, Telegrafenberg, 14473 Potsdam, Germany
[8]Physikalisches Institut, Heidelberg University, Im Neuenheimer Feld 226, 69120 Heidelberg, Germany
[9]Physikalisches Institut, University of Bonn, Nussallee 12, 53115 Bonn, Germany
[10]Institute of Geography, University of Augsburg, Alter Postweg 118, 86159 Augsburg, Germany
[11]Department of Hydrology and Water Resources, University of Arizona, 1133 E. James E. Rogers Way, 85721-0011 Tucson, Arizona, USA
[12]Institute of Experimental and Applied Physics, University of Kiel, Leibnizstraße 11, 24118 Kiel, Germany
[13]Helmholtz Zentrum München, Institute of Radiation Medicine, Ingolstädter Landstraße 1, 85764 Neuherberg, Germany

Correspondence: Benjamin Fersch (fersch@kit.edu)

Abstract.

Monitoring soil moisture is still a challenge: it varies strongly in space and time and at various scales while ~~well established~~ conventional sensors typically suffer from a small spatial support. With a sensor footprint up to several hectares, Cosmic-Ray Neutron Sensing (CRNS) is ~~an emerging~~ a modern technology to address that challenge.

So far, the CRNS method has typically been applied with single sensors or in sparse national scale networks. This study presents, for the first time, a dense network of 24 CRNS stations that covered, from May to July 2019, an area of just 1 km²: the pre-alpine Rott headwater catchment in Southern Germany which is characterized by strong soil moisture gradients in a heterogeneous landscape with forests and grasslands. With substantially overlapping sensor footprints, ~~that~~ this network was

5

1

designed to study root zone soil moisture dynamics at the catchment-scale. The observations of the dense CRNS network were complemented by extensive measurements that allow users to study soil moisture variability at various spatial scales: roving (mobile) CRNS units, remotely sensed thermal images from Unmanned Areal Systems (UAS), permanent and temporary wireless sensor networks, profile probes as well as comprehensive manual soil sampling. Since neutron counts are also affected by hydrogen pools other than soil moisture, vegetation biomass was monitored in forest and grassland patches, as well as meteorological variables; discharge and groundwater tables were recorded to support hydrological modeling experiments.

As a result, we provide a unique and comprehensive ~~dataset~~ data set to several research communities: to those who investigate the retrieval of soil moisture from cosmic-ray neutron sensing, to those who study the variability of soil moisture at different spatio-temporal scales, and to those who intend to better understand the role of root-zone soil moisture dynamics in the context of catchment and groundwater hydrology, as well as land – atmosphere exchange processes. The data set is available through the EUDAT Collaborative Data Infrastructure (EUDAT), and is split into two subsets: https://doi.org/10.23728/b2share.282675586fb94f44ab2fd09da0856883 (Fersch et al., 2020a) and https://doi.org/10.23728/b2share.bd89f066c26a4507ad654e994153358b (Fersch et al., 2020b).

1 Introduction

1.1 The relevance of soil moisture observation

Soil moisture is a key state variable of the Earth's environmental system, controlling various processes at various scales: the exchange of water and energy between the land surface and the atmosphere, runoff generation and groundwater recharge, vegetation development and growth in natural and managed systems, or the release of greenhouse gases from soils.

But while soil moisture is a much desired quantity in research and applications, its observation remains a challenge (Beven et al., 2020; Ochsner et al., 2013). Numerous techniques exist for measuring soil moisture at specific points in space, including vertical profiles, such as ~~TDR, FDR~~Time Domain Reflectometry (TDR), Frequency Domain Reflectometry (FDR), and soil sampling. While these techniques all have specific uncertainties and limitations – including even the benchmark standard technique of thermo-gravimetry – they share one fundamental limitation: the uncertain spatial representativeness. This shortcoming results from the small support volume (footprint of the measurement in the order of centimeters) in combination with the strong and potentially abrupt variation of soil moisture in space (Blöschl and Grayson, 2000). This issue can be overcome by very dense ~~in-situ~~ in situ sensor networks (see, e.g., Bogena et al., 2010). At the other end of the scale continuum, remote sensing techniques allow for a higher spatial coverage and a volume- or area-integrated measurement approach. Wang and Qu (2009) and Mohanty et al. (2017) provide an overview of techniques based on optical, thermal, passive microwave, and active microwave measurements. Yet, apart from the fact that these are indirect observations and are thus inherently uncertain, they typically have limited (and often imprecisely characterized) penetration depths that cannot be assumed to be representative

40 for the root zone. Over densely vegetated terrain the uncertainty of these remote sensing techniques increases. Furthermore, both airborne and spaceborne remote sensing of soil moisture often come along with infrequent measurement intervals due to a limited overpass frequency.

1.2 Cosmic ray neutron sensing of soil moisture

Cosmic-Ray Neutron Sensing (CRNS) is a ~~promising~~ modern measurement technique to close the scale gap in soil moisture
45 observation. According to simulations by Köhli et al. (2015), the sensor can provide volume-integrated soil moisture estimates with an exponentially-shaped horizontal footprint of hundreds of meters (the "plot scale") and a vertical footprint of tens of centimeters, corresponding to the upper root zone. Bogena et al. (2013) and Schrön et al. (2018) showed that the temporal resolution of standard detectors is in the range of 3 to 12 hours and strongly depends on the detector technology used. The principles of the CRNS method were introduced about twelve years ago by Zreda et al. (2008), followed by Desilets et al.
50 (2010), who presented the first results using mobile measurements and a conversion procedure to obtain soil moisture. Zreda et al. (2012) presented a complete overview over the method and the then newly established CRNS network in the USA. Andreasen et al. (2017) published a short synthesis of recent advancements in CRNS at that time, but soon afterwards important updates with respect to snow detection (Schattan et al., 2017) and road effects on roving CRNS measurements (Schrön et al., 2018) were published.

55 The CRNS sensor is sensitive to the ambient density of neutrons in the near-surface atmosphere. The main source of cosmic-ray induced neutrons exhibits energies between 10^5 and 10^9 eV (Köhli, 2019). Their interaction in the ground leads to neutrons in the energy range of 10^{-2} to 10^7 eV, of which epithermal neutrons (1–10^5 eV) are most sensitive to hydrogen and water (Zreda et al., 2012; Köhli et al., 2015). Hence, standard CRNS sensors are equipped with a polyethylene shield that reduces the thermal neutron (< 1 eV) fraction and slows down faster neutrons to detectable energies (Köhli et al., 2018). Some CRNS sensors
60 employ an additional "bare" counter which is sensitive to thermal neutrons only.

To date, a wide range of neutron detectors optimized for soil moisture monitoring exists ~~, using~~ and these use various gases or coating materials for neutron detection. An overview of detectors used in our field campaign is provided in section 3.4. For a detailed description of the technical components that make up standard CRNS units, including detector, telemetry, and additional atmospheric sensors, the reader is referred to Zreda et al. (2012) and Schrön et al. (2018).

65 The intensity of detected neutrons is mainly controlled by the interaction with hydrogen pools in the sensor footprint, of which soil moisture is typically the most important, though not the only one. A standard approach to estimate the gravimetric (θ_{grv}) or volumetric soil moisture (θ_{vol}, often referred to as θ) from epithermal neutron count rates N is to use the transfer function proposed by Desilets et al. (2010):

$$\theta_{\mathrm{grv}} = \frac{a_0}{N/N_0 - a_1} - a_2\,, \quad \theta_{\mathrm{vol}} = \frac{\varrho_b}{\varrho_w} \cdot \theta_{\mathrm{grv}} \tag{1}$$

70 In that form, the transfer function requires the calibration of parameter N_0 once, in order to take the specific measurement conditions into account. The value not only depends on the local terrain features, soil moisture heterogeneity, and instru-

mental sensitivity (Schrön et al., 2018), but also on the local prevalence of other hydrogen pools, such as vegetation, litter, soil organic carbon, and lattice water (Andreasen et al., 2017). The ~~shape~~ parameters a_0, a_1, and a_2 ~~could be adapted to specific local conditions, but they have also proven~~ have proved to be robust in ~~many previous studies~~ their original formulation across multiple CRNS sites (Desilets et al., 2010; Evans et al., 2016; Schrön et al., 2017, among others), while few locations apparently work better with different values (Rivera Villarreyes et al., 2011; Iwema et al., 2015; Heidbüchel et al., 2016). Soil bulk density ϱ_b (kg/m^3) needs to be measured or estimated locally, while the density of water, ϱ_w, can be assumed to be 1000 kg/m^3.

The calibration of N_0 requires the availability of soil moisture observations within the horizontal and vertical footprint of the sensor. Schrön et al. (2017) have synthesized the state-of-the-art methodology on how to make use of distributed point-scale soil moisture measurements for sensor calibration and proposed adequate sampling designs.

Yet, calibration can only account for the effect of static hydrogen pools at a specific point in time, while hydrogen pools such as vegetation are typically dynamic. In addition, the collection and processing of soil samples for measuring thermo-gravimetric soil moisture is particularly labour-intensive.

One of the challenges in using CRNS for soil moisture observation is thus to separate the part of the signal that is related to soil moisture from those parts affected by other hydrogen pools such as vegetation and soil organic carbon (Baatz et al., 2015; Andreasen et al., 2017; Jakobi et al., 2018). Further prerequisites include the correction of atmospheric effects such as air pressure, air humidity, and fluctuations of incoming neutron radiation (Rosolem et al., 2013; Schrön et al., 2016; Hawdon et al., 2014), and a better, physically-based understanding of the spatial sensitivity of the neutron sensors, both vertically and horizontally, and how it is influenced by dynamic environmental conditions in the footprint (Köhli et al., 2015; Schrön et al., 2017; Schattan et al., 2019).

While the horizontal footprint of a single CRNS sensor already exceeds the spatial support of conventional techniques, further attempts have been made to enhance the spatial coverage ~~:~~ such as *roving CRNS* and *networks of CRNS sensors*. The term *Roving CRNS* ~~involves~~ stands for the utilization of mobile CRNS sensors ~~, have~~ to increase the spatial extent of soil moisture measurements. It has been recognized as a promising approach to increasing the spatial scale ~~(see, e.g., Chrisman et al., 2013)~~ (see, e.g., Chrisman and Zreda, 2013). Within a CRNS roving campaign, the sensor unit is moved (e.g., by car) within the area of interest in order to explore the catchment-scale wetness conditions and related spatial patterns (Dong et al., 2014; Franz et al., 2015; McJannet et al., 2017; Schrön et al., 2018). Under ~~ideal situations~~ suitable conditions, up to hundreds of square kilometers may be covered in a single day. This coverage makes CRNS roving ~~a promising~~ an ideal method for closing the critical scale gap in soil moisture monitoring toward the scale of small to medium catchments. However, roving relies on campaign-based measurements and thus produces snapshots only. As roving requires neutron measurements with much higher temporal resolution (in the order of minutes), a CRNS rover usually consists of several larger detectors, resulting in an increase in achievable neutron count rates compared to stationary applications. In this context, an increase ~~of~~ in detector sensitivity would constitute a promising perspective: obviously, the potential to increase the signal-to-noise ratio by integrating neutron counts over time is limited if the sensor is mobile (Jakobi et al., 2020).

In contrast, *networks of CRNS sensors* operate multiple stationary CRNS-sensors. Some initiatives have established national CRNS monitoring networks with the aim of supporting environmental monitoring at larger scales. These networks are being implemented under the acronym of COSMOS (the COsmic-ray Soil Moisture Observing System). The first network was established in the USA by the University of Arizona and has already deployed more than 60 CRNS sensors at various locations across the USA (Zreda et al., 2012). The Australian network was supported by the CSIRO research institute and consists of nine sensors distributed across the continent under different environmental conditions (Hawdon et al., 2014). A network has also been established in the United Kingdom by the CEH (?)(Evans et al., 2016). Similar initiatives have been started in Kenya and India (Montzka et al., 2017). Yet, these networks aim at distributing single CRNS sensors at a national scale, similar to the idea of climate stations, providing localized measurements in a sparse network that spans large scales.

To better cover the spatial and temporal scales, the combination of both stationary and roving approaches has been explored (Chrisman and Zreda, 2013; Franz et al., 2015): a limited number of stationary sensors have been used to detect the temporal dynamics while roving surveys have provided the means for extra- and interpolation beyond the stationary sensors. Despite the promising results, many challenges have been identified due to the heterogeneity of land surface conditions and the validity of assumptions that govern the integration of roving CRNS data, which are sparse in time, with stationary CRNS data, which are sparse in space.

1.3 The Cosmic Sense Joint Field Campaign in 2019

The Cosmic Sense Research Unit, funded by the German Research Foundation (DFG), addresses the above challenges in a concerted effort with a consortium of eight German partner institutions. In this context, one component of the Cosmic Sense project is the targeted joint operation of a large number of CRNS sensors in a dense observational network. The scientific aims behind these "Joint Field Campaigns" (JFCs) are

- to systematically explore, at the landscape level, the effect of heterogeneity of soil and vegetation in the CRNS footprint on the neutron signals;

- to investigate the consistency of signals obtained from CRNS sensors of different manufacturers and sensitivities;

- to monitor water storage in the root zone, as the most dynamic storage component in a catchment, and to possibly assimilate these observations in a hydrological model;

- to establish a network with overlapping horizontal CRNS footprints in order to investigate the potential of constraining soil moisture estimates in space and time and thus to establish space-time representations of soil moisture at a resolution higher than the resolution of a single sensor;

- to better understand the influence of hydrogen pools other than soil moisture on the CRNS signal, and to develop corresponding correction procedures;

- to evaluate the relation between the spatial and temporal dynamics of CRNS footprints and thermal infrared remote sensing imagery.

5

As mentioned in the previous section, networks of a large number of CRNS sensors ~~had~~ have been established before; however, as sparse national scale networks they are not geared towards the scientific subjects elaborated above. Hence, the joint operation of 24 CRNS sensors that took place from early May to late July 2019, is unprecedented in its scope as it features a large number of detectors in an area of just $1\,km^2$, characterised by pronounced soil moisture gradients and heterogeneous land cover. The CRNS monitoring network was complemented by various observational techniques including CRNS roving, thermal imaging from Unmanned Aerial Systems (UAS), multiple FDR-sensor networks (SoilNet clusters) and profile probes, as well as manual measurements with FDR probes and thermo-gravimetry; and, finally, embedded in an established long-term observation infrastructure (TERENO Zacharias et al., 2011) and multiple synchronous observational campaigns (MOSES, ScaleX, see Sect. 4.1) that focused on water and energy fluxes in the atmospheric boundary layer. The observational period from late spring to midsummer was characterized by pronounced soil moisture dynamics, starting out from fully saturated conditions after persistent heavy rainfall, followed by more than two months of drying, occasionally interrupted by brief but intense rainfall events.

In this paper, we present this unique data set as a contribution to the CRNS community, but also to those researchers interested in exploring the potential of dense volume-integrated soil moisture observations from a hydrological perspective. The data set was split into two subsets and is freely available from EUDAT at (https://doi.org/10.23728/b2share.282675586fb94f44ab2fd09da0856883, and (https://doi.org/10.23728/b2share.bd89f066c26a4507ad654e994153358b, Fersch et al., 2020b).

We start by providing a detailed overview and justification of the choice of the study area (section 2). Section 3 constitutes the core of this paper: the presentation of the data collected as part of the JFC. Section 3.1 gives an overview of the various components, section 3.2 documents the underlying data model, and the subsequent sections describe these data sets in more detail. Section 4 outlines relevant data from third parties which ~~however~~ where not collected as part of the JFC, and are not part of this data publication. As this paper is about the presentation of the data set, we will not provide any further analysis or interpretation. However, in section 5, we will illustrate how the neutron count rates of stationary and roving sensors can be used to represent temporal soil moisture dynamics at the catchment scale, including the areal average of soil moisture and its variability in space. Based on that example, section 6 will conclude by outlining the potential of the presented data set.

2 Study site

In the selection process for the field campaign's study location the requirements of the different involved research projects needed to be reconciled. Important criteria were ~~backbone~~ long-term climate and soil-moisture observations, contiguous land-cover, good accessibility by foot and car for the mobile applications, a substantial fraction of nonforested area for the remote sensing (UAS) campaigns, shallow and time-variable groundwater levels, and a self-contained hydrological catchment to enable hydrological modeling. With the $1\,km^2$ Rott headwater catchment (Fig. 1), part of the Pre-Alpine Terrestrial Environmental Observatory ~~(TERENO, Kiese et al., 2018)~~ (TERENO Pre-Alpine Observatory, Kiese et al., 2018) of the Helmholtz association, we ~~could identify~~ identified a suitable candidate. The TERENO Pre-Alpine Observatory is situated about 50 km southwest of Munich, Bavaria, Germany and encompasses the $600\,km^2$ Ammer and the $55\,km^2$ Rott watersheds.
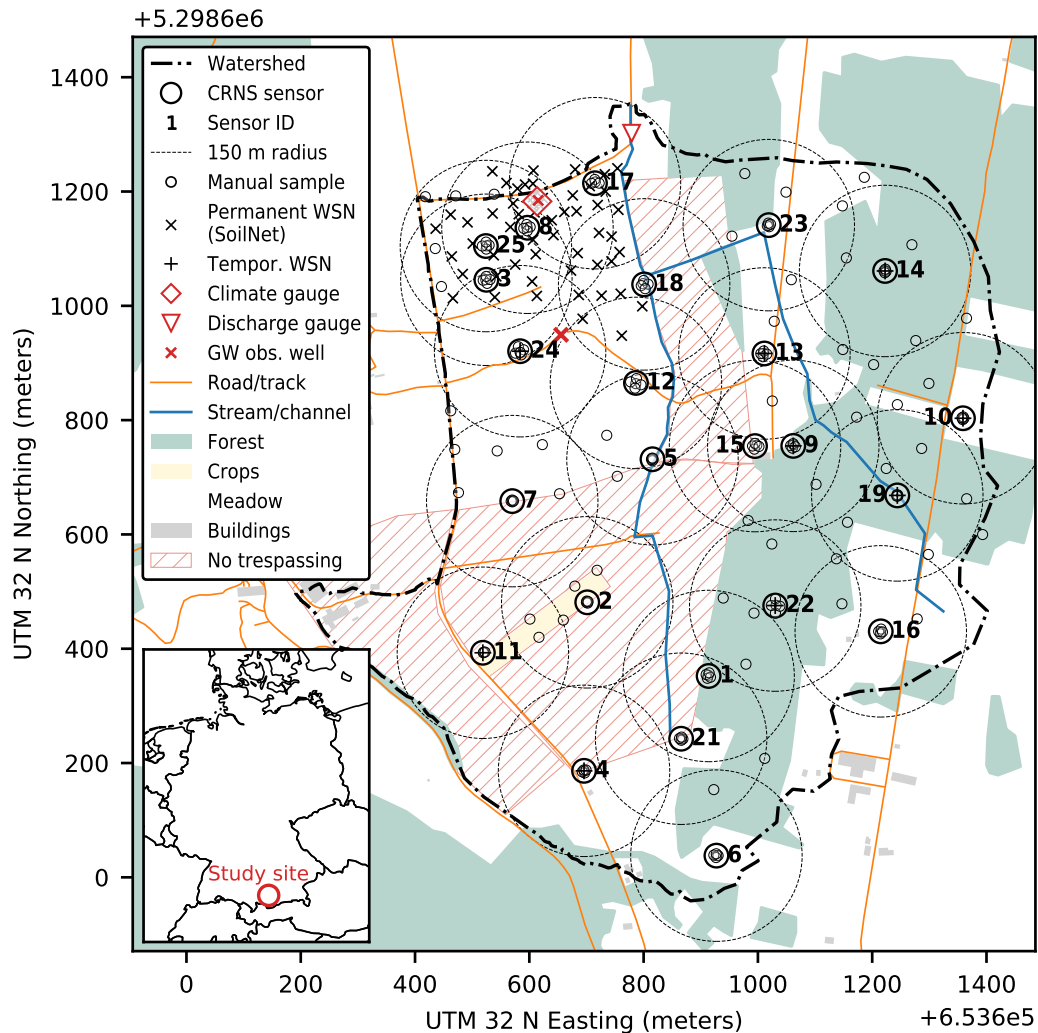
Figure 1. The Rott headwater catchment in Fendt near Peißenberg, Bavaria, Germany: the map shows the most important features of the study area and the JFC. In terms of land use, we only highlight forested area and a patch of cropland – the remaining parts are mainly meadows or grassland, with some scattered settlements – as well as roads and streams. In terms of instrumentation, we focus on showing the locations of the CRNS sensors with a 150 m radius as a typical footprint size for a medium level of soil moisture (Schrön et al., 2017), the climate station, and soil moisture profiles from SoilNet nodes and manual sampling on June 25–26, 2019. Basemap data from OSM (OpenStreetMap contributors, 2019), see section 4.4.

The Fendt site of the TERENO Pre-Alpine Observatory (595 m ASL) is located in the Rott headwater catchment. In the area, several multi- and interdisciplinary campaigns as well as some long-term ecological experiments were being carried out over the past years (e.g., SCALEX, Wolf et al., 2016; Kiese et al., 2018). Time-limited campaigns such as the JFC of Cosmic Sense

can help to complement the long-term observations at the TERENO Pre-Alpine Observatory locations, whereas on the other
hand they can build on preexisting knowledge and measurements.

The younger morphodynamics of the region were governed by glacial and post-glacial processes of the Quaternary. The
shallow, U-shaped valley of the Rott was carved into older sediments (molasse) by the Isar-Loisach glacier about 25 ~~k~~ thousand
years ago and this was followed by kettle lake sedimentation and fluvial erosion processes. Whereas towards the side slopes
of the valley gravels mixed with loamy and silty fractions are predominant, we find mainly silty and loamy sediments at the
lower elevations with peaty compositions towards the draining rivulet (Fersch et al., 2018).

In the Rott headwater catchment, between the deeper Tertiary (molasse) and the Quaternary sedimentation layers, shallow
aquifers have formed with hydraulic heads that range between 4 and 0.2 m below ground from the margins to the center of the
headwater catchment. The prevalent soil class is Cambic Stagnosol, which originated from the glacial parent material. Typical
clay, silt, and sand fractions are 32, 41, and 27 % (Kiese et al., 2018). We present a description of soil properties including
bulk density, lattice water content, organic matter and texture for composites in subsection 3.8. As can be seen from Fig. 1, the
landcover of the headwater catchment consists mainly of grassland, with some wetter regions along the creeks of the northern
part, and a forest on the eastern slope consisting of stands of coniferous or deciduous species with heterogeneous age.

The boundaries of the Rott headwater catchment were delineated according to the surface topography (DEM1 1 m x 1 m,
https://www.ldbv.bayern.de). For the subsurface (groundwater) we assume additional contributions from the adjacent hillslopes
to the west.

3 Methods and data

3.1 Overview

This section describes the measurements conducted during the campaign. Other complementary data are described in section 4.

The core innovation and overall motivation of this data set is the use of a dense network of 24 CRNS sensors in a study area
of roughly 1 km^2. These instruments of various types and their key observational variables are described in Tab. 2.

Around this core data set we carried out various measurements that are required to utilize, study and evaluate observed
neutron counts from the CRNS network for the purpose of soil moisture retrieval: meteorological observations (section 3.3);
soil properties and soil moisture measurements for calibration and validation, obtained at selected points and various depths
using different techniques (section 3.8); CRNS roving data (section 3.6) and remotely sensed thermal images (section 3.10),
both from several campaigns in order to obtain additional information on soil moisture variability in space; and measurements
and estimates of above-ground biomass (section 3.9) in order to account for the corresponding hydrogen pools in the CRNS
data analysis.

3.2 Data formats

The data presented in this study consist, for large parts, of time series data recorded at well-defined, sparse and static points in space (e.g., neutron counts, meteorological variables, soil moisture or permittivity). For such data, we decided to implement a simple, transparent, and easy-to-use data model that is based on standard text tables (character (tabulator) separated values, csv): each sensor (or sensor unit) is characterized in attribute tables, including a unique identifier (ID), location (latitude and longitude in WGS 84 reference system), measurement depth or height (in meters above or below the surface), and a set of sensor specific attributes that are documented in the attribute table's header. The time series of observations are provided in additional text tables: each sensor is represented by one file that is named according to the unique sensor ID. The first column in any such file holds the datetime (UTC, ISO 8601). Any other columns represents the measured variables which are documented in the file header, including the physical units.

Timeseries data with a fixed spatio-temporal resolution (e.g., data from SoilNet) are provided in NetCDF files which include an explicit documentation of all dimensions and observational variables, but which are also accompanied by an overview text table that contains key attributes of the measurement locations.

Any exceptions from these data models (e.g., for the CRNS roving, the land use and soil data, the digital elevation model, or the remote sensing data) are explicitly elaborated in the corresponding subsections, and by using meta data files. For polygon data, we use the ESRI shapefile and the geojson format, for gridded data the GeoTIFF format.

~~Please see~~ Further details of the data repository are given in section 7.

3.3 Meteorological data

The permanent ~~backbone~~ meteorological instrumentation at the Rott headwater catchment (also known as the TERENO site Fendt) consists of an eddy-covariance flux tower and several precipitation sensors. Besides the high frequency measurements of the eddy-flux system (the data of which is available through the Integrated Carbon Observation System ICOS and TERENO), standard climate variables are recorded every minute. The meteorological observations and their respective devices selected for the presented data set are listed in Tab. 1.

3.4 Stationary CRNS data

During the period from mid-May to mid-July 2019, a total of 24 stationary CRNS sensors were operated, though not all sensors were measuring at all times. CRNS sensor #8 in the north-east had already been installed as part of TERENO infrastructure, and continued operation after the JFC. The temporal data availability is illustrated in Fig. 9, center panel. Data gaps and differing periods of data availability are due to various reasons, including different dates for installation/deinstallation, sensor maintenance, power failures, or logger configuration, to name a few.

Tab. 2 gives an overview of all stationary CRNS sensors that were used during the campaign. Fig. 2 illustrates the proportions of the different sensor models. Out of the 24 sensors, 18 have been manufactured by Hydroinnova LLC (Albuquerque, NM, USA). Those instruments are based on neutron-sensitive detector gases, which are either ^{3}He gas (CRS-1000, CRS-2000) or

Table 1. Meteorological instrumentation in the Rott headwater catchment (instrumentation is part of the TERENO Pre-Alpine Observatory at the Fendt site).

Variable	Sensor Brand	Accuracy	Precision
air temperature	WXT520, Vaisala	$\pm$ 0.3 °C	0.1 °C
air rel. humidity	WXT520, Vaisala	$\pm$ 3 %	0.1 %
air pressure	WXT520, Vaisala	$\pm$ 5 mbar	1 mbar
global radiation	SPN1, DeltaT Devices	$\pm$ 8 %	0.6 W m^2
precipitation	Pluvio^2, Ott Hydromet	$\pm$ 1 %	0.01 mm
wind speed	WXT520, Vaisala	$\pm$ 3 %	0.1 m s^{-1}
wind direction	WXT520, Vaisala	$\pm$ 3°	0.1°

235   ^{10}BF$_3$ enriched gas (CRS-1000-B, CRS-2000-B). Five sensors (StX-140-5-15) were manufactured by StyX Neutronica GmbH (Dossenheim, Germany), and feature a new experimental design, based on solid ^{10}B-lined converters. One of the 24 sensors was manufactured by Lab-C LLC (Tucson, AZ, USA), and also constitutes a new approach that uses a multi-wire proportional chamber with solid ^{6}Li as a neutron converter. Fig. 3 exemplifies time series of raw neutron count rates from six CRNS sensors of different types (manufacturers) and thus different sensitivities.

240   For all CRNS sensors, the detection chamber is surrounded by a so-called moderator material in order to "thermalize" (i.e. slow down) epithermal neutrons for detection (see Zreda et al., 2012; Schrön et al., 2018; Köhli et al., 2018, for details). Six sensor units were equipped with an additional detection unit without a moderator (i.e. a "bare counter") in order to directly count thermal neutrons (see Tab. 2). This approach was motivated by recent studies which show that the ratio of thermal to epithermal neutron count rates is useful to distinguish specific hydrogen pools, namely vegetation biomass (Tian et al., 2016;

245 Jakobi et al., 2018) or snow (Schattan et al., 2017).

   The CRNS sensor units were equipped with varying meteorological sensors for air temperature, relative humidity and air pressure, all of which are required to correct for atmospheric effects on epithermal neutron count rates. For some units, such sensors were only available internally in the logger box (making the observations less representative for the sensor footprint), while some units also featured external meteorological sensors. A more detailed specification of the placement of meteorolog-

250 ical sensors is included in the metadata of the individual CRNS sensor units. All CRNS sensors were set up to record neutron counts and additional variables at a temporal interval of 20 minutes.

   At 19 of the 24 CRNS sensor locations a profile probe (40 or 100 cm maximum measurement depth, see section 3.8.3 for further details) was installed to monitor the vertical distribution of soil moisture.

   The locations of the CRNS sensors are shown in Fig. 1. The sampling design underlying the placement of sensor units was

255 subject to various scientific and practical – partly antagonizing – constraints:

- to achieve a maximum coverage of the catchment area in order to capture soil moisture storage dynamics in the root zone as an important dynamic part of the catchment's water balance and a key control of groundwater recharge;

Table 2. Overview of CRNS sensors installed during the JFC, including: manufacturer, model, and converter technology; the availability of standard moderated detector tubes for epithermal neutrons (mod) and additional bare tubes for thermal neutron detection (bare); the dominant land cover in the footprint of the sensor; the maximum measurement depth of co-located profile probes near the CRNS sensor; the sensitivity factor (ratio between raw neutron counts of the individual sensor and the calibrator unit (#20).

ID	Manufacturer	Sensor model	Technology	Tubes	Dominant land cover	Profile depth	Sensitivity
1	Hydroinnova	CRS 2000-B	$^{10}BF_3$	mod & bare	forest, meadow	100 cm	1.190
2	Hydroinnova	CRS 1000	^{3}He	mod	crops, meadow	100 cm	0.452
3	Hydroinnova	CRS 1000	^{3}He	mod & bare	meadow	–	0.458
4	Lab-C	NeuSens dual	^{6}Li	mod	meadow	100 cm	4.530
5	Hydroinnova	CRS 1000-B	$^{10}BF_3$	mod	meadow	100 cm	0.670
6	Hydroinnova	CRS 1000-B	$^{10}BF_3$	mod	meadow, forest	100 cm	0.668[*]
7	Hydroinnova	CRS 1000-B	$^{10}BF_3$	mod	meadow	100 cm	0.668[*]
8	Hydroinnova	CRS 2000-B	$^{10}BF_3$	mod & bare	meadow	–	1.161
9	StyX Neutronica	StX-140-5-15	^{10}B	mod	forest, meadow	100 cm	–
10	StyX Neutronica	StX-140-5-15	^{10}B	mod	meadow, forest	100 cm	–
11	StyX Neutronica	StX-140-5-15	^{10}B	mod	crops, meadow	100 cm	–
12	StyX Neutronica	StX-140-5-15	^{10}B	mod	meadow	100 cm	–
13	StyX Neutronica	StX-140-5-15	^{10}B	mod	meadow	40 cm	0.984
14	Hydroinnova	CRS 2000	^{3}He	mod	forest	100 cm	0.871
15	Hydroinnova	CRS 2000	^{3}He	mod	meadow, forest	100 cm	0.871[*]
16	Hydroinnova	CRS 2000-B	$^{10}BF_3$	mod & bare	meadow	40 cm	1.148
17	Hydroinnova	CRS 2000-B	$^{10}BF_3$	mod & bare	meadow	–	1.121
18	Hydroinnova	CRS 1000	^{3}He	mod & bare	meadow	100 cm	0.414
19	Hydroinnova	CRS 2000-B	$^{10}BF_3$	mod	forest	40 cm	1.147[*]
20	Hydroinnova	Calibrator	^{3}He	mod	–	–	1.000
21	Hydroinnova	CRS 2000-B	$^{10}BF_3$	mod	meadow, forest	100 cm	1.132
22	Hydroinnova	CRS 2000-B	$^{10}BF_3$	mod	forest	40 cm	1.168
23	Hydroinnova	CRS 2000-B	$^{10}BF_3$	mod	meadow, forest	40 cm	1.127
24	Hydroinnova	CRS 2000-B	$^{10}BF_3$	mod	meadow	100 cm	1.138
25	Hydroinnova	CRS 1000-B	$^{10}BF_3$	mod	meadow	–	0.665

[*] No direct measurement available, values were obtained by using the average of same sensor models as a reference.

– antagonistic to the former, to achieve a maximum overlap of CRNS footprints in order to better constrain the estimation of soil moisture patterns in space and time from multiple CRNS signals;

– to achieve a balance of coverage between the different land cover and soil types, most notably with regard to 'meadow' versus 'forest' cover and 'loamy/silty' versus 'peaty' soils;

11
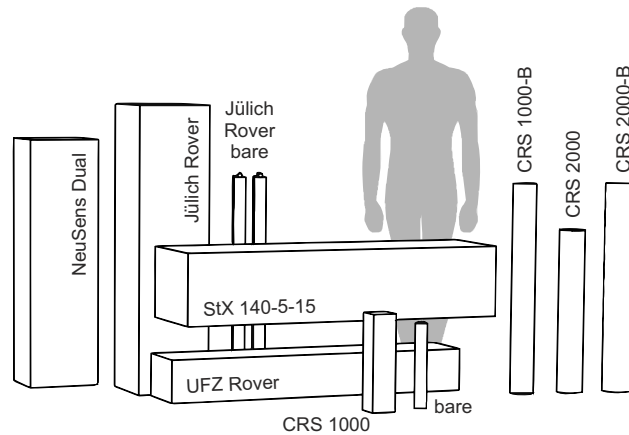
Figure 2. Dimension of CRNS sensors employed in the campaign. The blocks illustrate the size of the detectors; the actual units also comprise other components, combined in a slightly larger housing.

- to represent different positions along hill slopes inclined towards the northward draining rivulet;

- to avoid properties for which owners did not grant permission for trespassing nor installing equipment (mostly in the West-Southwest);

265

- to use locations with sufficient insolation for solar panels;

- to efficiently incorporate existing observational infrastructure (such as the SoilNet in the North-West);

- to keep a minimum distance of 15 meters to roads in order to minimize the effect of roads on CRNS measurements (Schrön et al., 2018);

- to ensure proximity to tracks for the installation of the heavy StX-140-5-15 units and to enable comparisons with the

270   cosmic rover measurements.

The trade-off between the aim of maximum coverage versus maximum overlap was resolved by increasing the density of CRNS sensors in the north west, where the permanent SoilNet allows for optimal validation.

3.5 Standardisation of neutron count rates

Neutron count rates at different observation locations were obtained with different CRNS sensor types. Even within the same
275   sensor type, the effective sensitivity varies. Between all sensors used in this study, the sensitivity between the least and the most sensitive sensor (CRS-1000 and Lab-C, respectively) is expected to vary by an order of magnitude. In order to compare neutron count rates observed at different locations, these count rates need to be normalized to a standard level. Given that the effective sensitivity of the instrument is unknown, we need to introduce a reference standard. For that purpose, we placed a mobile CRNS sensor ("calibrator", Hydroinnova, #20 in Tab. 2, basically consisting of two combined CRS-1000 systems) just
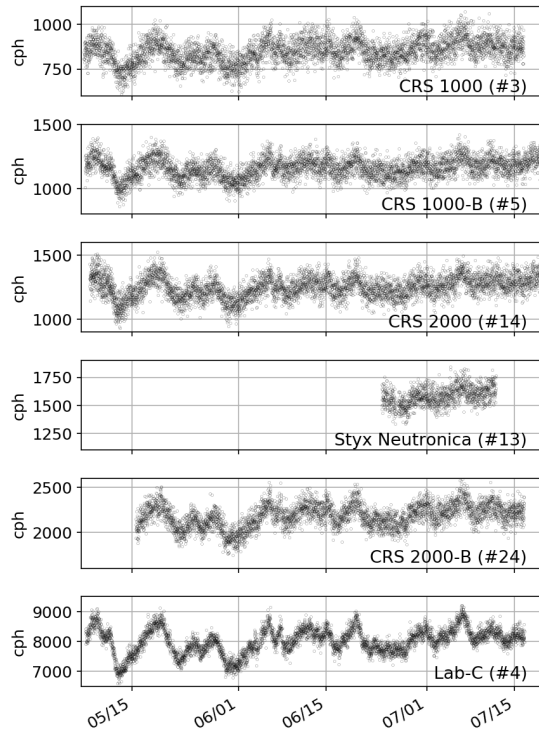
Figure 3. Raw (not standardized, uncorrected) neutron count rates (in counts per hour, cph) recorded at an integration interval of 20 minutes by six exemplary CRNS sensors representing different manufacturers/models (sensor ID in parentheses, see Tab. 2). While the qualitative dynamics are visually similar, the different sensitivities become evident by both different averages and different signal-to-noise ratios~~, please mind the different~~. Note: y-axis scaling differs between plots.

beside each stationary CRNS sensor for a period of at least 24 hours. The ratio between the average count rates of the stationary CRNS sensor and the calibrator - the sensitivity factor - was used to standardize the count rates for the entire time series to the calibrator level. For those CRNS sensors which we could not collocate with the calibrator, we used the average sensitivity factors obtained for the same instrument type. The resulting sensitivity factors are included in Tab. 2. Furthermore, a CRNS rover unit was collocated with most of the stationary CRNS sensors on June 27 which provides a further sensitivity reference (see section 3.6).

3.6 Roving CRNS

During the campaign, portable cosmic-ray neutron sensors were used:

- to study the spatial variability of neutron intensity and soil moisture in the whole catchment and particularly in-between the stationary sensors;

- to validate the spatial representativeness of the stationary sensors and its dependency on different land use types;

13

Figure 4. Inter-calibration of the stationary sensor (middle) using the mobile rover on a hand wagon (left) and the mobile calibrator unit (right), with minimum record periods of 20 min and 24 h, respectively.

– to investigate differences in the sensitivity of the stationary sensors by using the mobile sensor as a reference standard.

We used three types of mobile devices:

– UFZ rover (installed in a Land Rover Defender) equipped with a moderated CRNS-RV unit (Hydroinnova LLC, Albuquerque, USA) based on ^{3}He gas (see Schrön et al., 2018, for details). In contrast to previous studies, we applied an additional polyethylene shield of 5 cm thickness below the detector to reduce local effects. Air temperature and humidity were recorded with sensors attached outside the car. Three consecutive measurements underwent a moving-average filter to account for the moving footprint and to reduce the relative statistical uncertainty (Zreda et al., 2012; Jakobi et al., 2020) . The average epithermal neutron count rate across all campaigns was $9\,788 \pm 2\,141$ cph prior to corrections;

– hand wagon equipped with the identical detector system as in the UFZ rover (Fig. 4). This type of measurement has been applied mainly on June 27th for sensor intercalibration and to cross terrain that is inaccessible for cars. On a few days in May and June, the same measurement principle has been used for further sensor intercalibration;

– FZJ rover (Mercedes Sprinter) equipped with an array of nine neutron detector units (Hydroinnova LLC, Albuquerque, USA), each holding four tubes filled with ^{10}BF$_{3}$. During the campaigns, the rover was configured to measure epithermal neutrons with five detector units, three in vertical and two in horizontal orientation. The remaining four bare detector units measured thermal neutrons during the experiments to calculate the thermal-to-epithermal neutron ratio N_r (see, e.g., Tian et al., 2016; Jakobi et al., 2018). The average epithermal neutron count rate across all campaigns was $38\,919 \pm 5\,815$ cph prior to corrections;

14

All detector systems were set to integrate neutron counts over 10 seconds, and the driving speed ranged from 10 to 100 meters per minute. Within the two months of the field campaign, roving measurements took place on 13 days (see Fig. 6).

3.7 Local Neutron Monitor and Bonner Spheres

The neutron intensity at ground level strongly depends on the incoming cosmic-ray neutron flux. In order to account for variations of that incoming flux, researchers typically use neutron monitor (NM) recordings from the Neutron Monitor Database (http://www.nmdb.eu) as a baseline. For that purpose, Hawdon et al. (2014) and Schrön et al. (2016) recommended to select a neutron monitor with a cutoff rigidity similar to the study location. Consequently, we suggest neutron monitors Irkutsk and Jungfraujoch as potential candidates for the reference flux:

- Fendt site, $R_{\mathrm{cut}} = 4.14 \pm 0.02\,\mathrm{GV}$ (calculation based on Herbst et al., 2013), altitude $595\,\mathrm{m}$,

- Irkutsk NM, $R_{\mathrm{cut}} \approx 3.64\,\mathrm{GV}$, altitude $435\,\mathrm{m}$,

- Jungfraujoch NM, $R_{\mathrm{cut}} \approx 4.49\,\mathrm{GV}$, altitude $3570\,\mathrm{m}$.

Nevertheless, open questions about the suitability of neutron monitor data for local CRNS applications still exist, as pointed out by Schrön and Baroni et al. (2018). To build the basis for a more thorough analysis in future studies, we take advantage of additional neutron detector instruments during the study period in Fendt, the so-called Mini-NM (Krüger et al., 2008), and Bonner Spheres (Bramblett et al., 1960; Rühm et al., 2012). Both instruments were installed close to CRNS probe #15, and measure different neutron energies due to different thickness of the polyethylen shielding (PE).

Combinations of multiple Bonner spheres can be used to estimate the spectral flux distribution (i.e., the energy spectrum) of secondary cosmic-ray neutrons (Leuthold et al., 2007). The Bonner Spheres are spherical ^{3}He proportional counters (3.3 cm diameter, type SP9, Centronic Ltd.) surrounded by polythylene shields of 3, 5, ~~and~~ 6, 8, 9, 10, 12 inch, respectively. An additional bare detector without any surrounding material was used to get a high response to thermal neutrons. To increase the response to high-energy neutrons ($> 20\,\mathrm{MeV}$), the 9" detector has been modified by adding a 0.5" lead shell (Mares and Schraube, 1997). ~~Combinations of multiple Bonner spheres can be used to estimate the spectral flux distribution (i.e., the energy spectrum) of secondary cosmic-ray neutrons (Leuthold et al., 2007).~~

Figure 5 shows a comparison of the count rates from the remote neutron monitors at Jungfraujoch and Irkutsk, the local Mini-NM, and the local Bonner Spheres. Future studies will investigate the environmental factors that have an effect on the various neutron energies and which of the detectors is most suitable for the incoming neutron corrections.

3.8 Soil data and local soil moisture observations

As pointed out in section 1.2, the estimation of volumetric soil moisture from epithermal neutron count rates typically requires a sufficient number of soil moisture and bulk density measurements in the sensor footprint. These measurements commonly originate from thermo-gravimetry (the retrieval of soil moisture as the mass difference of a soil core before and after oven-drying),
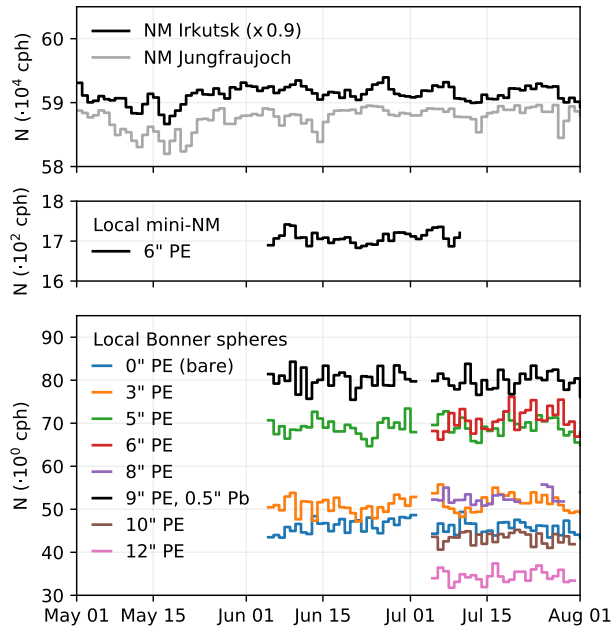
Figure 5. Neutron count rate N for different detector types: the remote neutron monitors at Jungfraujoch and Irkutsk, the local Mini-NM, and the local Bonner Spheres. Each instrument is equipped with different PE or lead shields to adjust the detection sensitivity towards different neutron energies.

but may as well be acquired with other measurement techniques. The more reference measurements within the footprint are available, the more reliably the effects of spatial variability of soil moisture can be accounted for in the calibration.

340   In this study, we combined several measurement techniques. The Rott headwater catchment study site at Fendt is partly equipped with permanent soil moisture measurement devices (SoilNet, see section 3.8.1, and Fig. 1), which provided long-term spatially- and temporally dense records. For the observation period, the existing network was temporarily extended by additional wireless sensors (see 3.8.2) and profile probes (see 3.8.3).

In addition to these continuous observations, manual sampling was carried out in an intensive campaign from June 25–26,
345   2019 (see section 3.8.4). In that campaign, soil samples were extracted directly at the sensor locations from various depths for the thermo-gravimetric measurement of water content and other soil properties. Furthermore, vertical profiles of FDR measurements were carried out at these and additional locations.

3.8.1   Permanent soil sensor network (SoilNet)

The permanent soil moisture monitoring data at Fendt are available since June 2015. In total, 55 vertical profiles were dis-
350   tributed in the north-west part of the Rott headwater catchment, covering an area of about 9 ha (Fig. 1). Each profile records permittivity, and temperature in 5, 20, and 50 cm depth, every 15 minutes. The system is an implementation of SoilNet (ver-
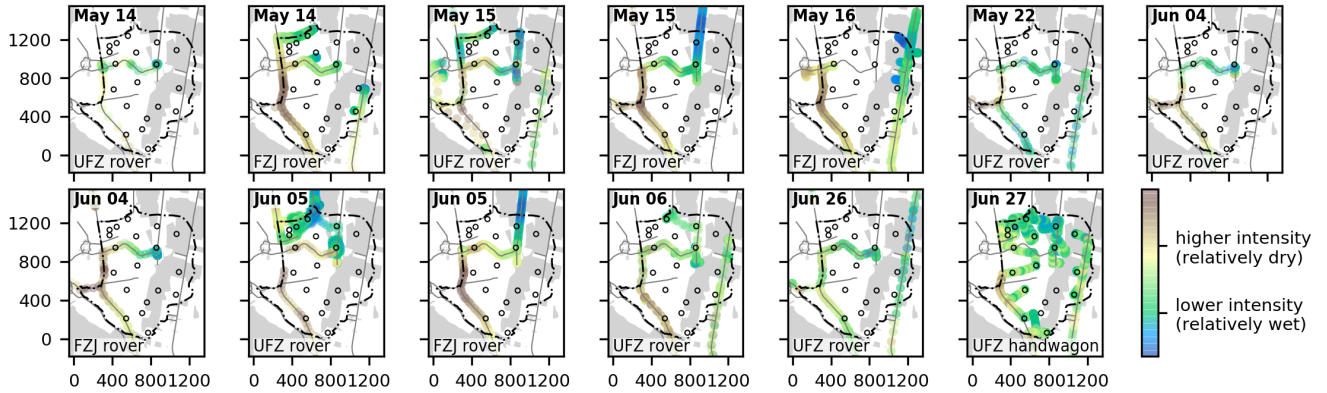
Figure 6. Roving tracks and relative neutron intensity. Each panel represents a roving campaign day and a rover type (UFZ rover, FZJ rover, handwagon). The color code qualitatively indicates the variability of observed corrected neutron intensity within a single roving campaign, where a higher neutron intensity corresponds to drier conditions. Forested and built-up areas as well as roads are shown in grey, the watershed is represented by the broken black line; stationary CRNS sensor locations by the sensor's ID. Basemap data from OSM (OpenStreetMap contributors, 2019), see section 4.4.

sion 3) - a ready-made system, developed at Forschungszentrum Jülich GmbH, Germany (SoilNet, 2018). Permittivity and temperature are measured redundantly at each depth with two slightly displaced sensors (SMT100, Truebner GmbH, Neustadt, Germany). The SMT100 uses a ring oscillator to determine the permittivity of the soil from the electromagnetic propagation velocity. The relation between sensor counts and permittivity ϵ was individually calibrated for each device prior to installation according to Bogena et al. (2017) and Qu et al. (2013). We used the dielectric mixing model of Birchak et al. (1974) to link ϵ with the volumetric water content (θ)

$$\theta = \frac{\epsilon^{0.5} - (1-n)\,\epsilon_s^{0.5} - n\,\epsilon_a^{0.5}}{\epsilon_w^{0.5} - \epsilon_a^{0.5}}. \tag{2}$$

ϵ_s, ϵ_a, and ϵ_w stand for the permittivities of the solid, air, and water component of the soil. n denotes the porosity of the soil. The permittivity of the air is defined with $\epsilon_a = 1$ and ϵ_w was computed from temperature T (in °C) according to Weast (1986) with

$$\begin{aligned}
\epsilon_w = 78.54 \cdot \big(& 1 - 4.579 \cdot 10^{-3}\,(T-25) \\
& + 1.19 \cdot 10^{-5}\,(T-25)^2 \\
& - 2.8 \cdot 10^{-8}\,(T-25)^3\big).
\end{aligned} \tag{3}$$

For the permanent installation area, the values for the solid permittivity $\epsilon_s = 3.29$ and the porosity of the soil $n = 0.63$ were derived from a laboratory analysis of nine representative soil samples, following the methodology proposed by Qu et al. (2016).

We provide the SoilNet data in a compressed binary netCDF-4 format. The 15-minute interval timeseries cover the period May 1st–July 31st. We stored each variable in a separate field with the dimensions *profile ID, depth, and time*. The geographical

17

locations of the profiles are also contained in the file thus enabling geostatistical analyses. We did not fill data gaps that resulted
370 from sensor malfunction or transmission errors.

3.8.2 Temporary soil sensor network

In addition to the permanent SoilNet we installed flexible variants of such a sensor system, the so-called "Wireless soil moisture sensor networks" (WSN, see also Schrön et al., 2018; Lausch et al., 2018). The system is an implementation of the BaseNet system (IMMS gGmbH, Ilmenau, Germany), developed in cooperation with the Helmholtz Centre for Environmental Research
375 (UFZ, Leipzig, Germany), and includes standard SMT100 probes (Truebner GmbH, Neustadt, Germany).

Across the catchment, nine locations were equipped with vertical measurement profiles: eight locations with two profiles each, and one location with four profiles (i.e. 18 profiles in total). The locations were chosen to cover different land use types and to closely accompany the CRNS sensors #4, #9, #11, #13, #14 (four profiles), #19, #22, and #24 (see Fig. 1). Soil permittivity and temperature are measured with slightly displaced sensors at 15, 30, and 45 cm depth and in intervals of 10 minutes.
380 The measuring principle and calibration procedure correspond to the explanations in section 3.8.1. The corresponding porosity values of the soil were derived from a laboratory analysis of two representative soil samples for 15 cm and 30 cm depth at each location. For the solid soil components, we assumed a permittivity of $\epsilon_s = 3.29$ following the considerations of section 3.8.1.

3.8.3 Soil moisture profile probes

Soil moisture profile probes were installed throughout the study area in order to monitor the vertical distribution of soil moisture
385 over time. The vertical distribution pattern is not only affecting the vertical CRNS footprint (Köhli et al., 2015), but ~~also allows to better constrain~~ it also informs about vertical water movement and thus groundwater recharge (Baroni et al., 2018).

We employed FDR-based profile probes PR2 of three variants (PR2/6 analogue, PR2/4 SDI, PR2/6 SDI, Delta-T Devices LLC, Cambridge, England, UK). These were installed in the direct vicinity of the 19 stationary CRNS sensors outside the SoilNet, at a maximum distance of 1.5 m. PR2/4 measures at 10, 20, 30, and 40 cm depth, PR2/6 additionally yields values for
390 60 and 100 cm depth. Tab. 2 specifies the maximum measurement depths covered at each CRNS location.

The voltage readings U_{raw} recorded every 20 min were corrected and processed as described in section 3.8.4, using the manufacturer's equation (Delta-T, 2016)

$$\sqrt{\epsilon} = 1.125 - 5.53\,U_c + 67.17\,U_c^{\,2} - 234.42\,U_c^{\,3}$$
$$+ 413.56\,U_c^{\,4} - 356.68\,U_c^{\,5} + 121.53\,U_c^{\,6} \tag{4}$$

395 and applying eq. (6) after manually removing spurious data.

3.8.4 Manual soil moisture observations and soil sampling

~~To increase~~ A large number of manual soil moisture measurements were carried out from June 25 to 26, 2019 and these were useful for increasing the spatial coverage of the continuously-recorded soil moisture data, ~~to enable~~ enabling the calibration of

the ~~sensors and also to obtain~~ moisture sensors and obtaining basic soil properties (bulk density, residual water content, organic matter content, texture)~~, a large number of corresponding measurements were carried out from June 25 to 26, 2019.~~

The standard method for measuring soil moisture and other soil properties is collecting soil cores from various depths, and analysing them with thermo-gravimetry (referred to as *thermo-gravimetric profiles* in the following). Yet, that approach is also the most labour-intensive. It was not possible to apply that sampling procedure at a sufficient number of locations within two days. Therefore, the thermo-gravimetric approach was complemented by FDR measurements at the same depths (referred to as *FDR profiles* in the following). While manpower limited the total number of sampled sites, access permission posed further restrictions on their spatial distribution (see Fig. 1).

Altogether, the following sampling design was applied during the intensive campaign: Within 2 m around each CRNS sensor, a *thermo-gravimetric profile* was collected (details below). In the direct vicinity, an *FDR profile* was collected as an additional reference (details below). Four FDR profiles, surrounding the CRNS sensor in all cardinal directions within 3–6 m distance, complemented the survey in the close proximity to the CRNS sensors. Finally, randomly selected locations (under the constraints of access permission and of accounting for different land cover types in the footprint) served for closing remaining gaps in the design. The resulting collection consisted of 23 thermo-gravimetric and 139 FDR profiles. All measurement locations were surveyed with DGPS.

For collecting a *thermo-gravimetric profile*, a pit was excavated. Soil cores were horizontally extracted with cylinders (4 cm height, 5.6 cm diameter), at depths of 0 to 25 cm with an increment of 5 cm, where the measurement depth signified the distance between the soil surface and the upper edge of the sampling ring. Two replicate cores were extracted for each depth in each pit. Water content was determined by drying the samples at a temperature of 105 °C, and subsequent weighing. Analyses of residual water content and organic matter were performed for composite samples from three classes: (1) "forest" on "mineral" soil, (2) "other land use" on "mineral", or (3) "other land use" on "organic" soil. For each class, mixed samples for each 5-cm-increment served for analyses, which consisted of exposing the samples to 400 and 1000 °C for 16 and 12 h, respectively. For the mineral composite samples, a texture analysis was conducted using wet sieving and laser diffraction (Helos, Sympatec GmbH, Germany).

The *FDR profile* resulted from handheld ML2 ThetaProbes (Delta-T Devices LLC, Cambridge, UK) performed in vertically-augered holes of incrementally increasing depths. The depth increments of 5 cm correspond to those of the thermo-gravimetric measurements. Here, the depth refers to the upper end of the electrodes after the probe had been fully inserted. At each depth, the probe was vertically inserted, read, and extracted three times, with a slight rotation after each time, in order to capture micro-scale variability. Sensor voltage U_{raw} served as the primary variable recorded. Since U_{raw} varied considerably between individual sensors, each reading was linearly converted to corrected voltage U_c. This conversion was based on sensor-specific calibration performed in air and water. The resulting corrected values of U_c allowed their conversion to permittivity ϵ according to manufacturer's specifications (Delta-T, 1998):

$$\sqrt{\epsilon} = 1.07 - 6.4 U_c + 6.4 U_c{}^2 - 4.7 U_c{}^3. \tag{5}$$

We tested various published equations for converting ϵ to the θ determined from thermo-gravimetry at the points of concomitant measurements. Since none of the tested relations performed satisfactorily, we re-fitted the coefficients of these equations. The best fit was achieved with the re-adjusted equation of Zhao et al. (2016) resulting in

$$\theta = \frac{-0.3846\,\varrho - 1.1037 + \sqrt{\epsilon}}{-2.2595\,\varrho + 1.7629 + (0.8995\,\varrho + 0.6479) \cdot \sqrt{\epsilon}}, \tag{6}$$

with ϱ being the dry bulk density in units of $\mathrm{g\,cm^3}$. The variable ϱ was related to the ϵ according to the respective soil stratum and depth layer as described above.

3.9 Vegetation and biomass

Cosmic ray neutron sensors are affected by all hydrogen pools within the footprint. Therefore, water stored in plants and hydrogen as a component of the plant tissue had to be quantified. The applied methods differ for grassland (more dynamic due to mowing operations) and forest (higher total biomass).

3.9.1 Biomass on grassland and cropland

Above-ground biomass on grass- and cropland sites was sampled three times (May 14–16, June 6 and July 17) at the same 45 locations (see Fig. 7). For that purpose, all plant material within a $30\,\mathrm{cm} \times 30\,\mathrm{cm}$ frame was harvested and immediately weighed in the field, using a mobile scale. Subsequently, the samples were stored in labelled paper bags for transport to the lab and oven dried to constant weight at $65\,^{\circ}\mathrm{C}$.

The vegetation water content can be estimated from weight loss after drying. For the amount of hydrogen and oxygen stored in cellulose, Franz et al. (2013) suggested a stoichiometric approximation (55.6 %).

Most grassland patches experienced multiple farming operations during the campaign, namely mowing, drying of the cut grass, baling, and removal of hay. These operations generally took place on patches defined by their respective ownership. The status of these patches (see Fig. 7) was visually inspected every 3–4 days and recorded according to the above-mentioned stages. These records should allow assessing the effects of management on the above-ground biomass dynamics.

3.9.2 Biomass in forest

Woodland covers a considerable fraction of the study area. While this forest is largely dominated by spruce (*Picea abies*), it also hosts smaller groves or individual trees of beech (*Fagus sylvatica*), alder (*Alnus glutinosa*), and ash (*Fraxinus excelsior*). The heterogeneous age of the stands makes it more difficult to estimate forest biomass. The collected data are intended to enable composite methods for the estimation of biomass employing spectral and LIDAR-based (see 4.3) remote sensing imagery and tree inventory data (e.g., Brovkina et al., 2017).

Forest mapping consisted of a *plot-based* and a *tree-based* survey (for locations, see Fig. 7). The *plot-based* mapping provides ground-truth for species classification. We mapped the forested area during June-August 2019. We selected 29 sites consisting exclusively or largely of one tree species, and recorded species, position (handheld GPS), diameter of the patch and
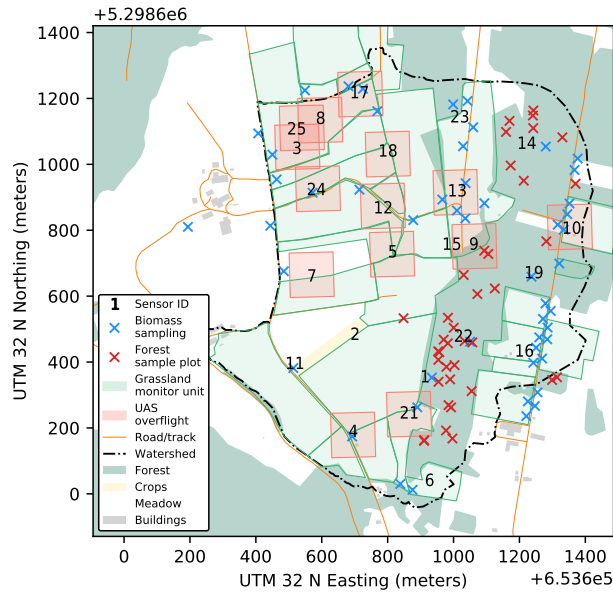
Figure 7. The layout of this figure corresponds to Fig. 1, but shows additional observation campaigns, namely the locations of vegetation biomass sampling (blue crosses, see section 3.9.1), areal units for monitoring the status of meadows (light green), forest/tree surveys (red crosses, see section 3.9.2), and UAS overflight zones (light red, see section 3.10). Basemap data from OSM (OpenStreetMap contributors, 2019), see section 4.4.

the approximate stand height (three measurements with laser rangefinder TruPulse 360B, LTI, Centennial, USA). The *tree-based* survey comprised four plots surveyed similarly to the method of Brovkina et al. (2017): within a circular plot of 25 m diameter, we recorded all single trees with at least 7 cm diameter, measuring their azimuth and distance from the centre of the plot, height (TruPulse 360B) and their circumference (tape measure) as a surrogate for breast-height-diameter.

Additionally, the forest undergrowth and litter mass was determined at six locations. For this purpose, all litter and plant material within a 30 cm × 30 cm frame was collected and processed in the same scheme as the crop- and grassland site samples (i.e. weighing in the field, oven-drying at 65 °C to constant weight). Water equivalents in undergrowth and litter mass were estimated by weight loss after drying summed with the stoichiometric amount of hydrogen and oxygen stored in cellulose (Franz et al., 2013, 55.6 %).

3.10 Thermal images from remote sensing

Thermal imagery was acquired covering a 60 m radius of 14 different CRNS sensors (see Fig. 7) as an indicator for soil moisture distribution within the footprint area of highest contribution to the CRNS signal (Köhli et al., 2015). The times and dates of every flight are summarized in Fig. 8.

475 For the data acquisition the UAS MK Okto XL 6S12 (HiSystems GmbH, Moormerland, Germany) equipped with a radio-
metric calibrated FLIR Tau 2 336 (FLIR Systems, Inc., Wilsonville, OR, USA) was used. This thermal camera uses a VOx
microbolometer focal plane array which is sensitive to wavelengths from 7.5–13.5 μm. Manufacturers specify an accuracy of
$\pm 5°$C. The camera was upgraded with an external shutter system (TeAx Technology UG, Wilnsdorf, Germany) to achieve a
better radiometric accuracy and avoid the vignetting effect in the individual scenes (personal communication R. Schlepphorst
480 2019, May 5). Further features are its 9 mm focal length and a sensor resolution of 336×256 pixels, leading to a $35° \times 27°$
field of view.

Flights were performed at an altitude of 100 m and a speed of approximately 5 m s^{-1} with a horizontal and vertical scene overlap
of 82 % $\times$ 84 %. Within each area of interest, five to ten ground control plates were distributed to enable accurate georectifica-
tion of the geomatic products. Their positions were determined with a Leica Zeno GG04 (Leica Geosystems AG, Heerbrugg,
485 Switzerland) DGPS antenna with sub-pixel accuracy.

Three steps of data preprocessing were performed before the creation of orthomosaics: For each individual scene capture,
the camera creates multiple frames. The frame with the highest image quality according to the Agisoft Image Quality tool ~~is~~
was selected for further processing. The extracted frames were temperature corrected as proposed by Maes et al. (2017)

$$T_{\text{UAScorr}} = T_{\text{UAS}} - T_{\text{air}} + T_{\text{air\_mean}}, \tag{7}$$

490 with T_{UAScorr} and T_{UAS} being the corrected and uncorrected measured temperature by the camera, respectively, T_{air} the air
temperature at the moment of image capture and $T_{\text{air\_mean}}$ the mean of the air temperature during the flight. Air temperature of
the meteorological data (see 3.3) served as input for the correction. The orthomosaics for each flight were created in Metashape
Professional (Version 1.5.3, Agisoft LLC, St. Petersburg, Russia). The application of a Wallis filter (Wallis, 1977) increased the
contrast within the individual frames and thus enabled automatic feature recognition by the image alignment algorithms. The
495 filtered images are again substituted by the temperature corrected frames when building the orthomosaic in 'mosaic' mode.
The RMSE of the positions of the ground control plates is included in the metadata of each flight.

3.11   Discharge

Discharge observations, which are, for example, needed for setting up hydrological or land surface models of the stuy area,
were derived from water level measurements (Datalogger Type 575-II, HT-Hydrotechnik, Obergünzburg, Germany), taken at
500 the outlet of the Rott headwater catchment in the north (see Fig. 1) with ten minutes resolution. The rating curve was derived
from salt-tracer–electric conductivity measurements. Due to the lack of discharge reference values for channel water levels
above 40 cm, discharge rates exceeding 0.1 m^3 s^{-1} are increasingly uncertain.

3.12   Groundwater levels

For hydrological modeling and water balance assessments, information about the groundwater dynamics are also of interest.
505 The saturated zone at the Fendt valley bottom can be differentiated into a shallow aquifer situated on top of and between the
Quaternary sediment layers and a thicker, deeper confined aquifer. For each groundwater layer, a hydraulic head measurement
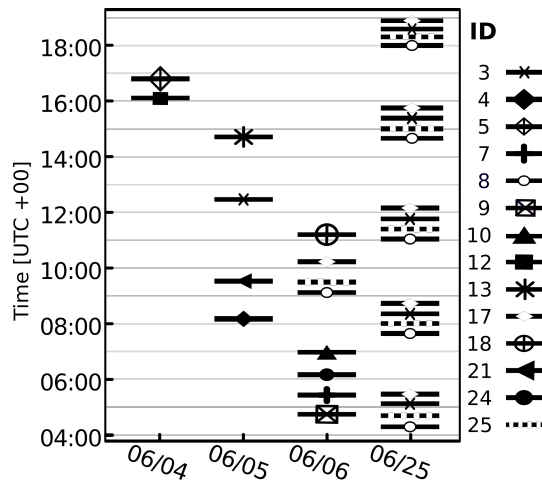
Figure 8. Summary of UAS flights. The areas correspond to the CRNS sensor ID (see Fig. 1). Every flight had a flight duration of approximately 10 minutes.

is available during the campaign period. The observation well for the shallow aquifer is located in the vicinity of the climate station, and the one for the deeper aquifer is situated below the country road, south of the SoilNet at the center between the CRNS sensors #12, #18, and #24 (see Fig. 1). The time series were recorded with three hourly (Datalogger Type 575-II, HT-Hydrotechnik, Obergünzburg, Germany) and 15-minute (Hobo U20L-04, Onset, Bourne, MA, USA) resolution for the shallow and deep aquifer, respectively. As the well opening for the shallow aquifer is flush with the ground surface and located in a small depression, strong precipitation events with ponding can cause a direct water flow into the well tube. Therefore, sharp peaks should be interpreted carefully and the groundwater temperature data should be considered as indicator for such events, too. Negative peaks in the time series are due to local pumping tests.

4   Related data from third parties

This section introduces several additional and useful data sets that are not part of this data publication, and are provided by institutions or research collaborators without direct involvement in the Cosmic Sense project.

4.1   Complementary data by ScaleX and MOSES heat wave campaign 2019

The Cosmic Sense joint field campaign 2019 was carried out at the same time as the ScaleX 2019 campaign of KIT Campus Alpin, which involved additionally the MOSES (Modular Observation Solutions for Earth System) test campaign for the heat wave event chain. From these activities, complementary measurements were performed including sensible and latent heat fluxes, net ecosystem exchange, turbulence statistics, planetary boundary layer depth, surface temperature, surface emissivity, surface thermal infrared images, vertical profiles of wind speed and direction, and water vapor and air temperature LIDAR

23

profiles at Hohenpeißenberg. As of now, access to this data needs to be requested from the individual project leaders of ScaleX 2019. Further description and contact information is available at https://scalex.imk-ifu.kit.edu.

4.2 Long-term hydro-meteorological observations

Long term hydrometeorological and ecological data for ~~TERENO Pre-Alpin~~ the TERENO Pre-Alpine Observatory and the Rott headwater catchment (Fendt) are available via the TERENO Data Discovery Portal (https://www.tereno.net/ddp/). Further details about the TERENO Pre-Alpine ~~observatory~~ Observatory are available in Kiese et al. (2018) and via the KIT Campus Alpin's website (https://www.imk-ifu.kit.edu/tereno.php.)

4.3 Digital Elevation Model and soil overview maps

A high-resolution digital elevation (DEM) or terrain model (DTM) can be helpful particularly for hydrological applications, e.g., for identifying flow paths or estimating the depth of the groundwater table, or for forest biomass estimation (see section 3.9). DEM and DTM products at various horizontal resolutions and vertical accuracy can be obtained from the corresponding state agency, the Bayerisches Landesamt für Digitalisierung, Breitband und Vermessung (https://www.ldbv.bayern.de), e.g., the DEM1 product with a resolution of $1\,m \times 1\,m$, and a vertical accuracy better than $20\,cm$.

Soil maps (Bodenübersichtskarte 1:25000) for Bavaria are available in vector (shapefile) format published under CC BY-3.0 license by the Bavarian Environmental Agency (LfU, https://www.lfu.bayern.de/umweltdaten/geodatendienste/pretty_downloaddienst.htm?dld=uebk25).

4.4 Land ~~cover~~ use, roads, waterways

During fieldwork and for visualisation, we used OpenStreetMap data layers (OpenStreetMap contributors, 2019) available via http://download.geofabrik.de, namely landuse, waterways, and traffic. The data are distributed under ODbL license (www.openstreetmap.org/copyright).

4.5 Meteorological data

The German Weather Service (DWD) provides open climate data via https://opendata.dwd.de. These include comprehensive open-access observations of climate variables at the climate station Hohenpeißenberg (identifier 2290, 977 m ASL) which is located about five kilometres south-west of the study area.

5 Example application

The prime motivation of this paper is to present a comprehensive data set to the scientific community. That data set provides all the information required to estimate, analyse and put into context spatio-temporal soil moisture patterns from different sensors, and at different scales.

5.1 The stationary CRNS network

The heart of the data set is the dense cluster of CRNS sensors. Although an in-depth data analysis is, by definition, beyond the scope of this data publication, we would still like to give an impression of the potential of this methodology as well as of the temporal and spatial variability of soil moisture in the context of this study. In order to convey such an impression, we applied a standard processing workflow to estimate soil moisture from neutron count rates. As we only consider this an "illustration", not a study result, we only briefly outline the corresponding steps in the following:

- **Standardize** neutron count rates to a common sensitivity level, which is the sensitivity of the calibrator sensor (see Tab. 2);

- **Correct** neutron count rates for the effects of incoming cosmic neutron flux, barometric pressure, and atmospheric water vapor. For that purpose, we applied the standard procedure summarized by Andreasen et al. (2017) in the section on "Correcting Neutron Intensity". To correct for the effects of pressure and water vapor, we used data from the climate gauge (see section 3.3) for all CRNS sensors; to correct for incoming neutron flux, we used the data from the neutron monitor at Jungfraujoch (see section 3.7);

- **Calibrate** the N_0 parameter from Eq. (1) for each CRNS sensor based on the soil moisture measurements obtained in the intensive manual sampling campaign (see 3.8.4). For computing the average observed soil moisture in a sensor footprint, we use the iterative horizontal and vertical weighting procedure suggested by Schrön et al. (2017);

- **Average** (or smooth) neutron count rates in time in order to increase the signal-to-noise ratio. In order to illustrate the behaviour over the entire study period, we applied a moving average with a window size of 24 hours; convert the smoothed neutron intensity to volumetric soil moisture using the calibrated N_0 and Eq. (1);

- **Interpolate** the soil moisture estimates $\theta_{\text{sensor},jk}$ obtained from each CRNS sensor j at each time step k to values at the pixel scale θ_{pixel}. For that purpose, we constructed a $10\,\text{m} \times 10\,\text{m}$ grid inside the spatial bounding box of the catchment. For each grid pixel i, a weight w_{ijk} was inferred for each CRNS sensor j from the value of the approximated horizontal weighting function as provided by Schrön et al. (2017), Eq. B1. Then, the soil moisture $\theta_{\text{pixel},ik}$ at each pixel i was computed as a weighted average based on Eq. (8):

$$\theta_{\text{pixel},ik} = \frac{\sum w_{ijk}\theta_{\text{sensor},jk}}{\sum w_{ijk}}. \tag{8}$$

It should be noted that the above processing workflow uses only parts of the entire data set in order to roughly characterise soil moisture patterns in space and time. The scientific potential of the data set, however, is in combining the various observations at various scales. ~~Yet,~~ Fig. 9 ~~already~~ illustrates the pronounced dynamics of soil moisture as well as the spatial variability, i.e. within the catchment area and over the campaign duration. From May 20 to 22, an unusually intense and persistent rainfall event resulted in more than 125 mm of rainfall in less than 48 hours, followed by another 40 mm towards the end of May. That
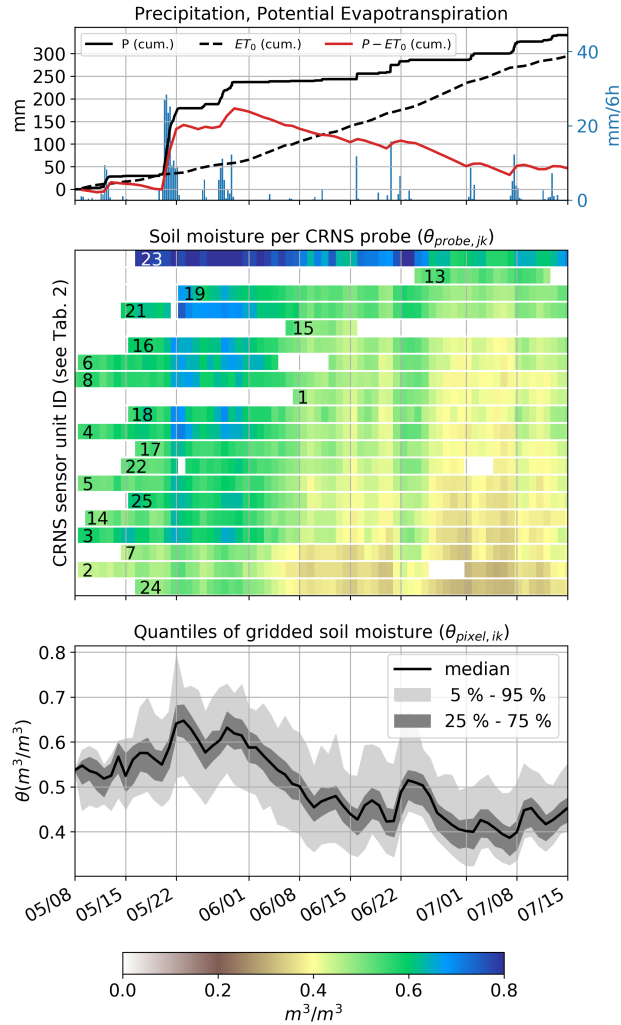
Figure 9. Dynamics of meteorological variables and soil moisture as estimated from neutron count rates. Upper panel: cumulative precipitation P, reference evapotranspiration ET_0 (FAO, 1998) based on Penman-Monteith, and the difference $P - ET_0$. Center panel: soil moisture $\theta_{\text{sensor},jk}$ estimated from neutron count rates for each of the CRNS sensors, where the sensors have been sorted from bottom to top in ascending order based on average soil moisture - the white spaces indicate periods of missing data; please note that the sensors #9–#12 are not included in this overview because they did not record valid data during the time of collocation with the calibrator sensor or the manual sampling campaign. Bottom panel: Temporal dynamics of different soil moisture quantiles after the soil moisture estimates have been interpolated to a grid (see main text to explanation).

sequence of events led to saturated conditions in the second half of May. Over June and July, the catchment was subject to substantial drying, interrupted by occasional, but intense rainfall events. The median volumetric soil moisture dropped from a maximum of 65 % to a minimum of 37 %. Over the same period, volumetric soil moisture always strongly varied in space: At

585 the driest period around early July, the wettest five percent of the catchment still exceeded a soil moisture of 45 %. The wettest parts of the catchment are located around CRNS sensor #23 (see Fig. 1 and 2) and are characterised by peat soils and very shallow groundwater tables.

5.2 Spatial patterns using mobile CRNS

The mobile roving campaign on June 27 (Fig. 6 and Fig. 10) brings the spatial patterns to a higher level of detail. The spatial
590 distribution of soil moisture in the Rott headwater catchment is ~~already~~ visible from the CRNS network, but only with the mobile measurements is it possible to cross the fields between the stationary sensors and to significantly extend spatial coverage and resolution. The campaign was conducted with the UFZ rover on a hand wagon and the data has been aggregated on a regular 30 m grid. Neutron data has undergone basic atmospheric corrections (see section 4.5), corrections for soil properties using the SoilGrids data base (Hengl et al., 2017; Fersch et al., 2018) and a reduction by 10 % at locations governed by forest-type land
595 use in order to account for the biomass effect (Baatz et al., 2015). The overall wetness gradient in the area has been confirmed, but the mobile measurements revealed a much larger wet spot in the north, which could not have been resolved by the stationary sensors due to a limited number of sensors located in that area. Besides the wet soil in the peat area and despite the downward shielding of the roving sensor, the observations are still clearly influenced by the lower water content of the roads which are typically slightly elevated over the surrounding areas (see Schrön et al., 2018, for a description of this effect). In prospective
600 analyses of the data for the determination of field soil moisture, it will be necessary to correct for this ,road effect', e.g., by applying the procedure developed by Schrön et al. (2018).

6 Conclusions

With this study, we present and provide a unique and comprehensive data set to several research communities: to those who investigate methods to retrieve soil moisture from cosmic ray neutron sensing, to those who study the variability of soil moisture
605 at different spatio-temporal scales, and to those who intend to better understand the role of root-zone soil moisture dynamics in the context of catchment and groundwater hydrology, as well as land-atmosphere exchange processes.

The data set is *unique* in that it involves, for the first time, a dense network of 24 CRNS sensors in a catchment area of $1\,km^2$. That catchment exhibited pronounced moisture gradients from wet peat to much drier loamy soils, and the campaign period was characterised by strong wetting and drying dynamics.
610 The data set is *comprehensive* in that it not only includes all the data that is required to interpret the neutron count rates from stationary sensors (meteorological time series, local soil moisture observations, soil properties such as bulk density and organic carbon content, and vegetation biomass), but also various rich data sets that allow users to put CRNS-based soil moisture estimates into various spatio-temporal contexts: CRNS roving campaigns, thermal imaging from multiple UAS overflights, multiple WSN clusters, as well as time series of discharge observations at the catchment outlet and groundwater levels.
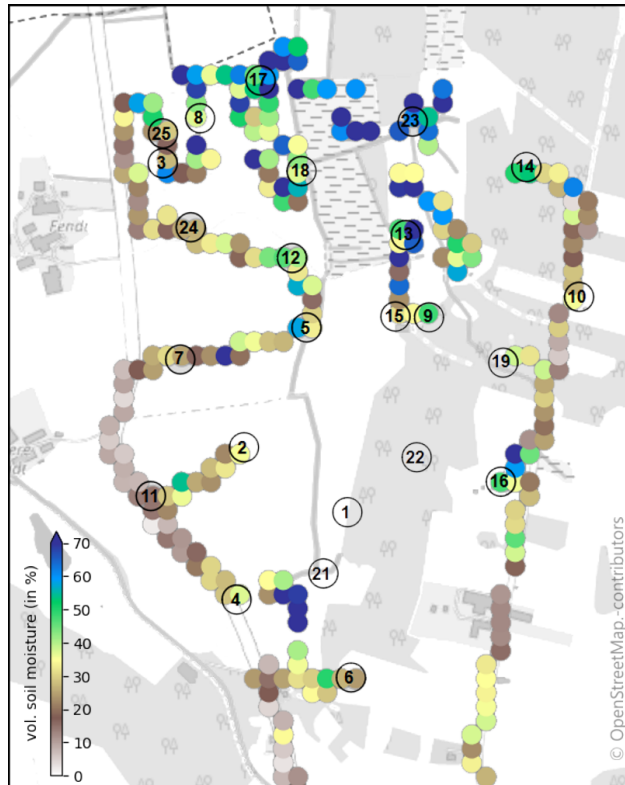
Figure 10. Roving with a hand wagon, passing every stationary sensor except #1, #21 and #22. Basemap © OpenStreetMap contributors 2020. Distributed under a Creative Commons BY-SA License.

In this way, the presented data set will be a valuable resource to those seeking a better understanding of cosmic ray neutron signals and for advancing scientific tools for CRNS-based soil moisture retrieval, and to those who aim to use these data and instruments for hydrological and hydrogeological applications.

7 Code and data availability

For data sharing and archiving we used the EUDAT Collaborative Data Infrastructure (https://eudat.eu). This pan-European e-infrastructure offers numerous data-related services ranging from sharing, archiving, processing to publication of the data. Its realization is closely related to the European Open Science Cloud (EOSC), a European initiative aimed at promoting free sharing of scientific data. In the context of this data publication, this project benefited from the services B2SHARE and B2HANDLE, both targeted at sharing, publishing and guaranteeing long-term persistence of data and managing persistent identifiers.

The data described in this paper are available from EUDAT ~~(Fersch et al., 2020a)~~ *Remark: These preliminary URIs are valid during the reviewing of this manuscript. They may need to be updated after the revision to a permanent URI*(https://doi.org/10.23728/b2share

. For more fine-grained access to the large files from the thermal imagery, these are hosted under a separate DOI ~~(Fersch et al., 2020b)~~ (https://doi.org/10.23728/b2share.bd89f066c26a4507ad654e994153358b, Fersch et al., 2020b) . The repository structure corresponds to the subsections of section 3 (see also Tab. 3). Besides the data, each folder contains a JSON-file (readable ASCII
630 text) holding meta data and additional format descriptions, where these differ from the conventions described in section 3.2.

Table 3. Overview of data categories and their path in the repository.

Section	Variable	Path in repository
3.3	meteo data	meteo.zip
3.4	CRNS-stationary	crns_stationary.zip/
3.6	CRNS-roving	crns_roving.zip
3.7	Neutron Monitors, Mini-NM, Bonner Spheres	crns_incoming.zip
3.8.1	soil moisture, permanent WSN[*]	soilmoisture_ permanent_wsn.zip
3.8.1	soil moisture, temporary WSN[*]	soilmoisture_ temporary_wsn.zip
3.8.3	soil moisture, profile probes	soilmoisture_ profile_probes.zip
3.8.4	soil properties, soil moisture, manual sampling	soilmoisture_ manual_sampling.zip
3.9	vegetation / biomass	biomass.zip
3.10	thermal imagery	(part II, separate DOI)
3.11	discharge	discharge.zip
3.12	groundwater	groundwater.zip

[*] Wireless soil moisture sensor network

We developed the R-package *FDR2soilmoisture*, ver. 0.107 (Francke, 2019) for processing the FDR-data, and made it freely available.

the planning of the campaign. Mandy Kasner, Amol Patil, Daniel Rasche, Lena Scheiffele, Jannis Weimar designed and conducted field-work as members of *Cosmic Sense*, Markus Köhli supported the data analysis. Tobias Gränzig conducted fieldwork and contributed to data processing; Christian Budach conducted a large share of the fieldwork; Sandra Szulc-Seyfried coordinated the campaign and participated in the fieldwork. Marek Zreda inspected the field site and served as an advisor. All authors contributed to the writing of the manuscript. Bernd Heber provided the Mini-NM and contributed to the analysis of its data. Ralf Kiese contributed to the conducting and analysis of the gravimetric soil sampling at Fendt. Vladimir Mares installed the Bonner Spheres and processed the data. Hannes Mollenhauer developed and installed the temporary wireless sensor networks and carried out the corresponding data processing. Ingo Völksch maintained the permanent soil moisture network at Fendt and processed the sensor data for publication together with Benjamin Fersch.

References

660   Andreasen, M., Jensen, K. H., Desilets, D., Franz, T. E., Zreda, M., Bogena, H. R., and Looms, M. C.: Status and Perspectives on the Cosmic-Ray Neutron Method for Soil Moisture Estimation and Other Environmental Science Applications, Vadose Zone Journal, 16, 1–11, https://doi.org/10.2136/vzj2017.04.0086, 2017.

Baatz, R., Bogena, H. R., Hendricks-Franssen, H.-J., Huisman, J. A., Montzka, C., and Vereecken, H.: An empirical vegetation correction for soil water content quantification using cosmic ray probes, Water Resources Research, 51, 2030–2046, 665   https://doi.org/10.1002/2014WR016443, 2015.

Baroni, G., Scheiffele, L. M., Schrön, M., Ingwersen, J., and Oswald, S. E.: Uncertainty, sensitivity and improvements in soil moisture estimation with cosmic-ray neutron sensing, Journal of Hydrology, 564, 873–887, https://doi.org/10.1016/j.jhydrol.2018.07.053, 2018.

Beven, K., Asadullah, A., Bates, P., Blyth, E., Chappell, N., Child, S., Cloke, H., Dadson, S., Everard, N., Fowler, H. J., Freer, J., Hannah, D. M., Heppell, K., Holden, J., Lamb, R., Lewis, H., Morgan, G., Parry, L., and Wagener, T.: Developing observational methods to drive fu-
670   ture hydrological science: Can we make a start as a community?, Hydrological Processes, 34, 868–873, https://doi.org/10.1002/hyp.13622, 2020.

Birchak, J. R., Gardner, C. G., Hipp, J. E., and Victor, J. M.: High dielectric constant microwave probes for sensing soil moisture, Proceedings of the IEEE, 62, 93–98, https://doi.org/10.1109/PROC.1974.9388, 1974.

Blöschl, G. and Grayson, R.: Spatial Observations and Interpolation, in: Spatial Patterns in Catchment Hydrology - Observations and Mod-
675   elling, edited by Blöschl, G. and Grayson, R., chap. 2, pp. 17–50, Cambridge University Press, Cambridge, 2000.

Bogena, H. R., Herbst, M., Huisman, J. A., Rosenbaum, U., Weuthen, A., and Vereecken, H.: Potential of Wireless Sensor Networks for Measuring Soil Water Content Variability, Vadose Zone Journal, 9, 1002–1013, https://doi.org/10.2136/vzj2009.0173, 2010.

Bogena, H. R., Huisman, J. A., Baatz, R., Hendricks-Franssen, H.-J., and Vereecken, H.: Accuracy of the cosmic-ray soil water content probe in humid forest ecosystems: The worst case scenario, Water Resources Research, 49, 5778–5791, https://doi.org/10.1002/wrcr.20463, 680   2013.

Bogena, H. R., Huisman, A. J., Schilling, B., Weuthen, A., and Vereecken, H.: Effective Calibration of Low-Cost Soil Water Content Sensors, Sensors, 17, 208, https://doi.org/10.3390/s17010208, 2017.

Bramblett, R. L., Ewing, R. I., and Bonner, T. W.: A new type of neutron spectrometer, Nuclear Instruments and Methods, 9, 1–12, https://doi.org/10.1016/0029-554X(60)90043-4, 1960.

685   Brovkina, O., Novotny, J., Cienciala, E., Zemek, F., and Russ, R.: Mapping forest aboveground biomass using airborne hyperspectral and LiDAR data in the mountainous conditions of Central Europe, Ecological Engineering, 100, 219–230, https://doi.org/10.1016/j.ecoleng.2016.12.004, 2017.

Chrisman, B. and Zreda, M.: Quantifying mesoscale soil moisture with the cosmic-ray rover, Hydrology and Earth System Sciences, 17, 5097–5108, https://doi.org/10.5194/hess-17-5097-2013, WOS:000329061400024, 2013.

690   Delta-T: ThetaProbe Soil Moisture Sensor Type ML2 User Manual (ML2-UM-1), Tech. rep., Delta-T Devices Ltd., 1998.

Delta-T: User Manual for the Profile Probe type PR2 (PR2-UM-5.0), Tech. rep., Delta-T Devices Ltd., 2016.

Desilets, D., Zreda, M., and Ferré, T. P. A.: Nature's neutron probe: Land surface hydrology at an elusive scale with cosmic rays, Water Resources Research, 46, W11 505, https://doi.org/10.1029/2009WR008726, 2010.

Dong, J., Ochsner, T. E., Zreda, M., Cosh, M. H., and Zou, C. B.: Calibration and Validation of the COSMOS Rover for Surface Soil Moisture 695   Measurement, Vadose Zone Journal, 13, 1–8, https://doi.org/10.2136/vzj2013.08.0148, 2014.

Evans, J. G., Ward, H. C., Blake, J. R., Hewitt, E. J., Morrison, R., Fry, M., Ball, L. A., Doughty, L. C., Libre, J. W., Hitt, O. E., Rylett, D., Ellis, R. J., Warwick, A. C., Brooks, M., Parkes, M. A., Wright, G. M. H., Singer, A. C., Boorman, D. B., and Jenkins, A.: Soil water content in southern England derived from a cosmic-ray soil moisture observing system – COSMOS-UK, Hydrological Processes, 30, 4987–4999, https://doi.org/10.1002/hyp.10929, 2016.

700 FAO: Crop evapotranspiration - Guidelines for computing crop water requirements - FAO Irrigation and drainage paper 56, Tech. rep., FAO, 1998.

Fersch, B., Jagdhuber, T., Schrön, M., Völksch, I., and Jäger, M.: Synergies for Soil Moisture Retrieval Across Scales From Airborne Polarimetric SAR, Cosmic Ray Neutron Roving, and an In Situ Sensor Network, Water Resources Research, 54, 9364–9383, https://doi.org/10.1029/2018wr023337, 2018.

705 Fersch, B., Francke, T., Heistermann, M., Schrön, M., and Döpper, V.: A massive coverage experiment of cosmic ray neutron sensors for soil moisture observation in a pre-alpine catchment in SE-Germany (part I: core data) [post-review version], https://doi.org/10.23728/b2share.282675586fb94f44ab2fd09da0856883, 2020a.

Fersch, B., Francke, T., Heistermann, M., Schrön, M., and Döpper, V.: A massive coverage experiment of cosmic ray neutron sensors for soil moisture observation in a pre-alpine catchment in SE-Germany (part II: thermal imagery) [post-review version], 710 https://doi.org/10.23728/b2share.bd89f066c26a4507ad654e994153358b, 2020b.

Francke, T.: FDR2soilmoisture: R-package for processing data of FDR-measurements to obtain soil moisture, https://github.com/TillF/FDR2soilmoisture, version: 0.106, 2019.

Franz, T. E., Zreda, M., Ferré, T. P. A., and Rosolem, R.: An assessment of the effect of horizontal soil moisture heterogeneity on the area-average measurement of cosmic-ray neutrons, Water Resources Research, 49, 6450–6458, https://doi.org/10.1002/wrcr.20530, 2013.

715 Franz, T. E., Wang, T., Avery, W., Finkenbiner, C., and Brocca, L.: Combined analysis of soil moisture measurements from roving and fixed cosmic ray neutron probes for multiscale real-time monitoring, Geophysical Research Letters, 42, 3389–3396, https://doi.org/10.1002/2015GL063963, 2015.

Hawdon, A., McJannet, D., and Wallace, J.: Calibration and correction procedures for cosmic-ray neutron soil moisture probes located across Australia, Water Resources Research, 50, 5029–5043, https://doi.org/10.1002/2013WR015138, 2014.

720 Heidbüchel, I., Güntner, A., and Blume, T.: Use of cosmic-ray neutron sensors for soil moisture monitoring in forests, Hydrology and Earth System Sciences, 20, 1269–1288, https://doi.org/10.5194/hess-20-1269-2016, 2016.

Hengl, T., Mendes de Jesus, J., Heuvelink, G. B. M., Ruiperez Gonzalez, M., Kilibarda, M., Blagotić, A., Shangguan, W., Wright, M. N., Geng, X., Bauer-Marschallinger, B., Guevara, M. A., Vargas, R., MacMillan, R. A., Batjes, N. H., Leenaars, J. G. B., Ribeiro, E., Wheeler, I., Mantel, S., and Kempen, B.: SoilGrids250m: Global gridded soil information based on machine learning, PLOS ONE, 12, 1–40, 725 https://doi.org/10.1371/journal.pone.0169748, 2017.

Herbst, K., Kopp, A., and Heber, B.: Influence of the terrestrial magnetic field geometry on the cutoff rigidity of cosmic ray particles, Annales Geophysicae, 31, 1637–1643, https://doi.org/10.5194/angeo-31-1637-2013, 2013.

Iwema, J., Rosolem, R., Baatz, R., Wagener, T., and Bogena, H. R.: Investigating temporal field sampling strategies for site-specific calibration of three soil moisture–neutron intensity parameterisation methods, Hydrology and Earth System Sciences, 19, 3203–3216, 730 https://doi.org/10.5194/hess-19-3203-2015, 2015.

Jakobi, J., Huisman, J. A., Schrön, M., Fiedler, J., Brogi, C., Vereecken, H., and Bogena, H. R.: Error Estimation for Soil Moisture Measurements With Cosmic Ray Neutron Sensing and Implications for Rover Surveys, Frontiers in Water, 2, 10, https://doi.org/10.3389/frwa.2020.00010, https://www.frontiersin.org/article/10.3389/frwa.2020.00010, 2020.

Jakobi, J., Huisman, J. A., Vereecken, H., Diekkrueger, B., and Bogena, H. R.: Cosmic Ray Neutron Sensing for Simultaneous Soil Water Content and Biomass Quantification in Drought Conditions, Water Resources Research, 54, 7383–7402, https://doi.org/10.1029/2018WR022692, 2018.

Kiese, R., Fersch, B., Bassler, C., Brosy, C., Butterbach-Bahlc, K., Chwala, C., Dannenmann, M., Fu, J., Gasche, R., Grote, R., Jahn, C., Klatt, J., Kunstmann, H., Mauder, M., Roediger, T., Smiatek, G., Soltani, M., Steinbrecher, R., Voelksch, I., Werhahn, J., Wolf, B., Zeeman, M., and Schmid, H.: The TERENO Pre-Alpine Observatory: Integrating Meteorological, Hydrological, and Biogeochemical Measurements and Modeling, Vadose Zone Journal, 17:180060, 1–17, https://doi.org/10.2136/vzj2018.03.0060, 2018.

Köhli, M.: The CASCADE ^{10}B thermal neutron detector and soil moisture sensing by cosmic-ray neutrons, Ph.D. thesis, doctoral thesis, Physikalisches Institut, Heidelberg University, https://doi.org/10.11588/heidok.00026969, 2019.

Köhli, M., Schrön, M., and Schmidt, U.: Response functions for detectors in cosmic ray neutron sensing, Nuclear Instruments and Methods in Physics Research Section A: Accelerators, Spectrometers, Detectors and Associated Equipment, 902, 184–189, https://doi.org/10.1016/j.nima.2018.06.052, 2018.

Köhli, M., Schrön, M., Zreda, M., Schmidt, U., Dietrich, P., and Zacharias, S.: Footprint characteristics revised for field-scale soil moisture monitoring with cosmic-ray neutrons, Water Resources Research, 51, 5772–5790, https://doi.org/10.1002/2015WR017169, 2015.

Krüger, H., Moraal, H., Bieber, J. W., Clem, J. M., Evenson, P. A., Pyle, K. R., Duldig, M. L., and Humble, J. E.: A calibration neutron monitor: Energy response and instrumental temperature sensitivity, Journal of Geophysical Research: Space Physics, 113, A8, https://doi.org/10.1029/2008JA013229, 2008.

Lausch, A., Borg, E., Bumberger, J., Dietrich, P., Heurich, M., Huth, A., Jung, A., Klenke, R., Knapp, S., Mollenhauer, H., et al.: Understanding forest health with remote sensing, part III: requirements for a scalable multi-source forest health monitoring network based on data science approaches, Remote sensing, 10, 1120, https://doi.org/10.3390/rs10071120, 2018.

Leuthold, G., Mares, V., Rühm, W., Weitzenegger, E., and Paretzke, H. G.: Long-term measurements of cosmic ray neutrons by means of a Bonner spectrometer at mountain altitudes–first results, Radiation protection dosimetry, 126, 506–511, https://doi.org/10.1093/rpd/ncm102, 2007.

Maes, W., Huete, A., and Steppe, K.: Optimizing the processing of UAV-based thermal imagery, Remote Sensing, 9, 476, https://doi.org/10.3390/rs9050476, 2017.

Mares, V. and Schraube, H.: High energy neutron spectrometry with Bonner spheres, in: Proceedings of the IRPA-Symposium, Radiation Protection in Neighbouring Countries of Central Eur. Prague, Czech Republic, pp. 8–12, http://www.iaea.org/inis/collection/NCLCollectionStore/_Public/30/031/30031609.pdf?r=1, 1997.

McJannet, D., Hawdon, A., Baker, B., Renzullo, L., and Searle, R.: Multiscale soil moisture estimates using static and roving cosmic-ray soil moisture sensors, Hydrology and Earth System Sciences, 21, 6049–6067, https://doi.org/10.5194/hess-21-6049-2017, 2017.

Mohanty, B. P., Cosh, M. H., Lakshmi, V., and Montzka, C.: Soil Moisture Remote Sensing: State-of-the-Science, Vadose Zone Journal, 16, vzj2016.10.0105, https://doi.org/10.2136/vzj2016.10.0105, 2017.

Montzka, C., Bogena, H. R., Zreda, M., Monerris, A., Morrison, R., Muddu, S., and Vereecken, H.: Validation of Spaceborne and Modelled Surface Soil Moisture Products with Cosmic-Ray Neutron Probes, Remote Sensing, 9, 103, https://doi.org/10.3390/rs9020103, 2017.

Ochsner, T. E., Cosh, M. H., Cuenca, R. H., Dorigo, W. A., Draper, C. S., Hagimoto, Y., Kerr, Y. H., Larson, K. M., Njoku, E. G., Small, E. E., and Zreda, M.: State of the Art in Large-Scale Soil Moisture Monitoring, Soil Science Society of America Journal, 77, 1888–1919, https://doi.org/10.2136/sssaj2013.03.0093, 2013.

OpenStreetMap contributors: Planet dump retrieved from https://planet.osm.org , https://www.openstreetmap.org, last access: 22-06-2020., 2019.

Qu, W., Bogena, H., Huisman, J., and Vereecken, H.: Calibration of a Novel Low-Cost Soil Water Content Sensor Based on a Ring Oscillator, Vadose Zone Journal, 12, vzj2012.0139, 1–10, https://doi.org/10.2136/vzj2012.0139, 2013.

775 Qu, W., Bogena, H. R., Huisman, J. A., Schmidt, M., Kunkel, R., Weuthen, A., Schiedung, H., Schilling, B., Sorg, J., and Vereecken, H.: The integrated water balance and soil data set of the Rollesbroich hydrological observatory, Earth System Science Data, 8, 517–529, https://doi.org/10.5194/essd-8-517-2016, 2016.

Rivera Villarreyes, C. A., Baroni, G., and Oswald, S. E.: Integral quantification of seasonal soil moisture changes in farmland by cosmic-ray neutrons, Hydrology and Earth System Sciences, 15, 3843–3859, https://doi.org/10.5194/hess-15-3843-2011, 2011.

780 Rosolem, R., Shuttleworth, W. J., Zreda, M., Franz, T. E., Zeng, X., and Kurc, S. A.: The effect of atmospheric water vapor on neutron count in the cosmic-ray soil moisture observing system, Journal of Hydrometeorology, 14, 1659–1671, 2013.

Rühm, W., Ackermann, U., Pioch, C., and Mares, V.: Spectral neutron flux oscillations of cosmic radiation on the Earth's surface, Journal of Geophysical Research: Space Physics, 117, A08 309, 1–9, https://doi.org/10.1029/2012JA017524, 2012.

Schattan, P., Köhli, M., Schrön, M., Baroni, G., and Oswald, S. E.: Sensing Area-Average Snow Water Equivalent with Cosmic-Ray Neutrons:
785 The Influence of Fractional Snow Cover, Water Resources Research, 55, 10 796–10 812, https://doi.org/10.1029/2019WR025647, 2019.

Schattan, P., Baroni, G., Oswald, S. E., Schoeber, J., Fey, C., Kormann, C., Huttenlau, M., and Achleitner, S.: Continuous monitoring of snowpack dynamics in alpine terrain by aboveground neutron sensing, Water Resources Research, 53, 3615–3634, https://doi.org/10.1002/2016WR020234, 2017.

Schrön, M.: Cosmic-ray neutron sensing and its applications to soil and land surface hydrology, Ph.D. thesis, Universität Potsdam, Germany,
790 223 pp., https://nbn-resolving.org/urn:nbn:de:kobv:517-opus4-395433, Access date: 22-06-2020, 2017.

Schrön, M., Zacharias, S., Köhli, M., Weimar, J., and Dietrich, P.: Monitoring Environmental Water with Ground Albedo Neutrons from Cosmic Rays, in: The 34th International Cosmic Ray Conference, vol. 236, p. 231, SISSA Medialab, https://doi.org/10.22323/1.236.0231, 2016.

Schrön, M., Zacharias, S., Womack, G., Köhli, M., Desilets, D., Oswald, S. E., Bumberger, J., Mollenhauer, H., Kögler, S., Remmler,
795 P., Kasner, M., Denk, A., and Dietrich, P.: Intercomparison of cosmic-ray neutron sensors and water balance monitoring in an urban environment, Geoscientific Instrumentation, Methods and Data Systems, 7, 83–99, https://doi.org/10.5194/gi-7-83-2018, 2018.

Schrön, M., Köhli, M., Scheiffele, L., Iwema, J., Bogena, H. R., Lv, L., Martini, E., Baroni, G., Rosolem, R., Weimar, J., Mai, J., Cuntz, M., Rebmann, C., Oswald, S. E., Dietrich, P., Schmidt, U., and Zacharias, S.: Improving calibration and validation of cosmic-ray neutron sensors in the light of spatial sensitivity, Hydrology and Earth System Sciences, 21, 5009–5030, https://doi.org/10.5194/hess-21-5009-
800 2017, 2017.

Schrön, M., Rosolem, R., Köhli, M., Piussi, L., Schröter, I., Iwema, J., Kögler, S., Oswald, S. E., Wollschläger, U., Samaniego, L., Dietrich, P., and Zacharias, S.: Cosmic-ray Neutron Rover Surveys of Field Soil Moisture and the Influence of Roads, Water Resources Research, 54, 6441–6459, https://doi.org/10.1029/2017WR021719, 2018.

SoilNet: SoilNet website, www.soilnet.de, Accessed on: 26-02-2020, 2018.

805 Tian, Z., Li, Z., Liu, G., Li, B., and Ren, T.: Soil water content determination with cosmic-ray neutron sensor: Correcting aboveground hydrogen effects with thermal/fast neutron ratio, Journal of Hydrology, 540, 923–933, https://doi.org/10.1016/j.jhydrol.2016.07.004, 2016.

Wallis, R.: A fast algorithm for space variant contrast stretching, in: 1977 11th Asilomar Conference on Circuits, Systems and Computers, 1977. Conference Record., pp. 240–245, IEEE, 1977.

Wang, L. and Qu, J. J.: Satellite remote sensing applications for surface soil moisture monitoring: A review, Frontiers of Earth Science in China, 3, 237–247, https://doi.org/10.1007/s11707-009-0023-7, 2009.

Weast, R. C., ed.: Handbook of Physics and Chemistry, CRC Press, Boca Raton, FL, USA, 67 edn., 1986.

Wolf, B., Chwala, C., Fersch, B., Garvelmann, J., Junkermann, W., Zeeman, M. J., Angerer, A., Adler, B., Beck, C., Brosy, C., Brugger, P., Emeis, S., Dannenmann, M., De Roo, F., Diaz-Pines, E., Haas, E., Hagen, M., Hajnsek, I., Jacobeit, J., Jagdhuber, T., Kalthoff, N., Kiese, R., Kunstmann, H., Kosak, O., Krieg, R., Malchow, C., Mauder, M., Merz, R., Notarnicola, C., Philipp, A., Reif, W., Reineke, S., Rüdiger, T., Ruehr, N., Schäfer, K., Schrön, M., Senatore, A., Shupe, H., Völksch, I., Wanninger, C., Zacharias, S., and Schmid, H. P.: The ScaleX campaign: scale-crossing land-surface and boundary layer processes in the TERENO-preAlpine observatory, Bulletin of the American Meteorological Society, 98, 1217–1234, https://doi.org/10.1175/bams-d-15-00277.1, 2016.

Zacharias, S., Bogena, H. R., Samaniego, L., Mauder, M., Fuß, R., Pütz, T., Frenzel, M., Schwank, M., Baessler, C., Butterbach-Bahl, K., Bens, O., Borg, E., Brauer, A., Dietrich, P., Hajnsek, I., Helle, G., Kiese, R., Kunstmann, H., Klotz, S., Munch, J. C., Papen, H., Priesack, E., Schmid, H. P., Steinbrecher, R., Rosenbaum, U., Teutsch, G., and Vereecken, H.: A Network of Terrestrial Environmental Observatories in Germany, Vadose Zone Journal, 10, 955–973, https://doi.org/10.2136/vzj2010.0139, 2011.

Zhao, Y., Ling, D.-s., Wang, Y.-l., Huang, B., and Wang, H.-l.: Study on a calibration equation for soil water content in field tests using time domain reflectometry, Journal of Zhejiang University-Science A, 17, 240–252, https://doi.org/10.1631/jzus.A1500065, WOS:000372318500006, 2016.

Zreda, M., Desilets, D., Ferré, T. P. A., and Scott, R. L.: Measuring soil moisture content non-invasively at intermediate spatial scale using cosmic-ray neutrons, Geophysical Research Letters, 35, L21 402, 1–5, https://doi.org/10.1029/2008GL035655, 2008.

Zreda, M., Shuttleworth, W. J., Zeng, X., Zweck, C., Desilets, D., Franz, T. E., and Rosolem, R.: COSMOS: the COsmic-ray Soil Moisture Observing System, Hydrology and Earth System Sciences, 16, 4079–4099, https://doi.org/10.5194/hess-16-4079-2012, 2012.